TURTLE TRACKING TROUBLE: THE INFLUENCE OF CARAPACE MORPHOLOGY AND COMPOSITION ON TRANSMITTER ADHESION TO LOGGERHEAD (*Caretta caretta*) SEA TURTLE KERATIN

A thesis submitted in partial fulfillment of the requirements for the degree

MASTER OF SCIENCE

in

MARINE BIOLOGY

by

KATHERINE M. HOFFMAN
MAY 2020

at

THE GRADUATE SCHOOL OF THE UNIVERSITY OF CHARLESTON, SOUTH CAROLINA AT THE COLLEGE OF CHARLESTON

Approved by:

Dr. Michael Arendt, Thesis Advisor

Dr. John Bowden

Dr. Gabriel Williams

Dr. John Zardus

Dr. Godfrey Gibbison, Interim Dean of the Graduate School

ABSTRACT

TURTLE TRACKING TROUBLE: THE INFLUENCE OF CARAPACE MORPHOLOGY AND COMPOSITION ON TRANSMITTER ADHESION TO LOGGERHEAD (*Caretta caretta*) SEA TURTLE KERATIN

A thesis submitted in partial fulfillment of the requirements for the degree

MASTER OF SCIENCE

in

MARINE BIOLOGY

by

KATHERINE M. HOFFMAN
MAY 2020

at

THE GRADUATE SCHOOL OF THE UNIVERSITY OF CHARLESTON, SOUTH CAROLINA AT THE COLLEGE OF CHARLESTON

Satellite telemetry provides spatial distribution data across populations and species. Multiple sea turtle studies indicate variability in track durations both within and between species. Intraspecies track duration disparities suggest possible effects of transmitter adhesion; thus, potential interactions between carapace morphology and composition on transmitter adhesion to loggerhead sea turtles scutes were evaluated. Epoxy adhesion strength across 143 scute subsamples ranged from 9 to 48 N, but was highly variable (CV = 0.4) and unrelated to scute attributes (Objective 1). Fatty acid profiles (FAP) from 64 scute subsamples across five individuals were generated using gas chromatography with flame ionization detection (Obj. 2). Scute total fat content was low (mean = 0.16%, maximum = 0.42%), and did not correlate with mean epoxy adhesion to corresponding scute subsamples (r = -0.4). Principal component analysis revealed long chain fatty acids drove separation in FAPs between individuals. Following identification of tile as a suitable substitute keratin substrate (Obj. 3), a laboratory study (Obj. 4) tested epoxy adhesion with respect to 0º vs. 30º shear angles (simulating carapace slope) and small vs. large epoxy footprints (simulating transmitter sizes). No detachments occurred for small (n = 10) or large (n = 10) transmitters at 0º at a maximum sustained force of 979 N for 20 minutes. Lastly, a field study evaluated the effects of biofouling and seawater submergence on surrogate transmitter retention (Obj. 5) for epoxy footprints and simulated carapace angles. Six of 20 small and two of 19 large transmitters detached from tile after 67 days, but results were not significantly different (P = 0.24) and no detachments occurred for angled samples (n = 40). Variability observed in epoxy adhesion to loggerhead keratin and early detachment of surrogate transmitters *in situ* suggest that transmitter detachment may be implicated in shorter track durations.

ACKNOWLEDGEMENTS

I would like to acknowledge my advisor, Dr. Michael Arendt, whose invaluable guidance aided me as I navigated the transition from student to scientist. I would also like to thank my committee members, Drs. John Bowden, Gabriel Williams, and John Zardus, for their creative input and constructive criticism. Special thanks to Christopher Evans, without whom this project would have never lifted off the ground, and to Dr. Michael Napolitano, who showed me the joy of chemistry.

Thanks to the South Carolina Department of Natural Resources and Hollings Marine Laboratory for providing space to conduct my research. I would like to extend my gratitude to the Marine Turtle Conservation Program, specifically Michelle Pate and Emma Schultz, for their assistance throughout my project and their continued kindness. I would like to thank Julianna Duran for her help in sample processing. Furthermore, thanks to members of the GPMB including Shelly Brew, Katie Hiott, Norma Salcedo, Pete Meier, and Greg Townsley for their support during my time at Grice Marine Lab.

Lastly, I give my deepest thanks to Addison, my friends, and my family; if not for your endless support and patience, my time in graduate school would have been far more difficult and far less rich. To my dad, Leo Hoffman II, I cannot say thank you enough for all you have taught me; you are my greatest role model. To my brother, Leo Hoffman III, thank you for challenging and inspiring me every day. And finally, to my mom, words cannot express how much I miss you. This would not be possible without you all.

TABLE OF CONTENTS

LIST OF FIGURES

LIST OF TABLES

CHAPTER 1. GENERAL INTRODUCTION

Satellite telemetry provides spatial distribution data across populations and species of sea turtles. Despite recent technological advances, several problems regarding track durations continue to arise for telemetry researchers. Previous studies have reported variability in track durations both within and between species of hard-shelled sea turtles (Mansfield *et al.*, 2009; Seney & Landry, 2011; Arendt, Segars, Byrd, Boynton, Whitaker, *et al.*, 2012). Intraspecies track duration disparities suggest possible effects of transmitter adhesion. As such, the present multidisciplinary study was initiated to assess the influence of the physical and biochemical properties of keratinous scutes as well as the mechanical properties of epoxy on transmitter adhesion to loggerhead (*Caretta caretta*) sea turtles. For the second chapter, the primary question addressed was whether scute composition affected epoxy adhesion strength. The third chapter was initiated to characterize the surface texture of loggerhead keratin, a crucial precursor for identifying suitable substitute materials for testing physical factors separate from biochemical composition. For the fourth chapter, the effects of carapace morphology and epoxy footprint on surrogate transmitter retention were evaluated. General conclusions were drawn and directions for future research were outlined in the fifth chapter of this study.

CHAPTER 2. EPOXY ADHESION AND SCUTE COMPOSITION

2.1. INTRODUCTION

To best inform natural resources management, population surveys must be designed with detailed knowledge of animal distribution patterns. Across terrestrial and marine species, temporal and spatial movement patterns for mobile organisms are monitored using several methodologies. Visual surveys are useful in terrestrial systems to document organism presence, but are of limited value in habitats where the ability to detect animals is obscured (Wilson, Hammond, & Thompson, 1997, 1999). Where visual capabilities are limited, physical capture provides a means for assessing distribution and an opportunity to evaluate site fidelity when mark-recapture methods are used (Bailey, 1951). Likewise, telemetry monitoring allows detailed tracking of animals following physical capture through use of devices that emit radio or sound waves (White & Garrott, 1990). Perhaps the greatest achievement in the telemetry field in recent decades is the automation of radio signal recording through geostationary orbiting satellites (Godley *et al.*, 2008) and vast arrays of *in situ* acoustic signal receivers (Welch *et al.*, 2009).

Advancements in satellite telemetry research have been achieved through a number of pioneer and modern techniques. Radio waves emitted from animal-borne transmitters have been tracked via the Advanced Research and Global Observation Satellite (ARGOS) across many species of highly mobile marine organisms, including

sea birds (Jouventin & Weimerskirch, 1990), marine mammals (McConnell *et al.*, 1992; Wood, 1998), and sea turtles (see review by Godley *et al.*, 2008). Satellite transmitter attachment techniques for sea turtles have varied over time, from tethering large, buoyant transmitter housings to the carapaces of nesting females (Stoneburner, 1982) to contemporary techniques of direct adhesion to the carapaces of hard-shelled species (Godley *et al.*, 2003; Seney *et al.*, 2010; Mansfield *et al.*, 2012). Harness attachments have enabled data collection for large, soft-shelled leatherback sea turtles (*Dermochelys coriacea*; Eckert & Eckert, 1986) and rapidly-growing juvenile hard-shelled sea turtles (Seney, Higgins, & Landry, 2010; Mansfield *et al.*, 2012). An additional advancement in this field is transmitter miniaturization to target small individuals (Hays, Bradshaw, James, Lovell, & Sims, 2007; Seney *et al.*, 2010). Such advancements have reduced drag, improved animal welfare, and presumably enhanced data quality (Watson & Granger, 1998; Godley *et al.*, 2003; Seney *et al.*, 2010; Mansfield *et al.*, 2012).

Despite recent advancements in this field, several problems regarding track durations continue to arise for satellite telemetry researchers. Among the hard-shelled sea turtle species commonly tracked in the southeastern U.S., satellite tracking durations are typically longer for loggerhead than for Kemp's ridley (*Lepidochelys kempii*) sea turtles (Table 2.1). Both species predominantly reside in near-shore and/or estuarine waters from spring through fall (Shoop & Kenney, 1992; Morreale & Standora, 2005; Arendt, Segars, Byrd, Boynton, Whitaker, *et al.*, 2012). Given overlap in generalized habitats and relatively standardized transmitter attachment methodologies across studies, intra- and inter-species track duration disparities warrant further investigation. Most hard-shelled sea turtle species inflict physical damage to transmitters (notably the signal antenna)

through wedging and grooming behavior against hard substrata (Caine, 1986; Seney, 2008). Track duration may also be compromised by biofouling, as barnacle accumulation on saltwater switches falsely indicates submergence and halts signal transmission to conserve battery life (Seney, 2008). Alternatively, since cured resins are chemically inert (M. Cribbs, personal communication, August 30, 2018) and likely do not interact with sea turtle keratin, epoxy adhesion may be affected by carapace composition and shear angle as a function of carapace curvature and transmitter placement. In addition, differences in keratin composition, documented among hoofed ungulates (Family Bovidae) and scaled sea turtles (Family Cheloniidae; Espinoza, Baker, & Berry, 2007), may conceivably introduce variability in epoxy adhesion.

The process of keratin formation in sea turtles is poorly understood, but studies with freshwater turtles suggest that the carapace consists of a thin, living epidermis connected to the skeleton and a thick, outer layer of predominantly corneous keratin firmly attached to the living epidermis (Alibardi & Toni, 2006b; Wang *et al.*, 2016). Keratin can be categorized into two groups: α-keratin that consists of larger diameter filaments organized in α-helices, and β-keratin that consists of thinner diameter filaments organized in β-pleated sheets (Wang & Sullivan, 2017). For hard-shelled freshwater turtles, the living dermis beneath the carapace consists almost entirely of β-keratin proteins that have a higher resistance to distension and can be more easily compacted due to their smaller size relative to α-keratins (Alibardi & Thompson, 1999; Alibardi & Toni, 2006a, 2006b). Generally, the carapace of freshwater turtles grows by enlarging and thickening the previous layer, while growing cells take up various amino acids along with calcium to synthesize β-keratin (Alibardi & Thompson, 1999; Alibardi & Toni, 2006b).

During the synthesis of keratin, freshwater turtles have specific organelles termed lamellar bodies that are particularly rich in polar lipids, glycolipids, and phospholipids, which are then transformed into more hydrophobic lipids that may contribute to the formation of a water-loss barrier (Alibardi & Toni, 2006a, 2006c).

The scute formation model for freshwater turtles suggests that composition of the outermost carapace layer may influence epoxy adhesion strength and duration for hard-shelled sea turtles. As such, the first question addressed in this study was whether scute composition affected epoxy adhesion in loggerhead sea turtles. For the first objective, epoxy adhesion was measured to assess intra- and inter-carapace differences. For the second objective, keratin fatty acid profiles were generated to characterize intra- and inter-carapace variability and to assess potential differences in molecular structure that may influence adhesion of a two-component marine epoxy widely used with loggerheads.

2.2. METHODS

Objective 1: Epoxy adhesion strength

The primary objective was to assess the break force (Newtons, N) of epoxy on loggerhead sea turtle scutes from different individuals and locations on the carapace. Pursuant to SCDNR Marine Turtle Conservation Program (MTCP) permit MTP-2018-0010, scutes were sampled from stranded individuals that expired from acute causes. Body condition scores of stranded individuals that were considered reasonable for inclusion in this study were obtained from MTCP records as follows: 0 = alive (when found), 1 = fresh dead, and 2 = moderately decomposed. To discourage scavenger interference during scute detachment, carcasses were placed outside in a metal wire

drying cage (173 cm length × 61 cm width × 61 cm height; Figure 2.1). Intact left costal, vertebral, and right costal scutes (maximum 15 scutes per individual) were collected following ≥24 hours of carcass drying, placed in uniquely labeled plastic bags, then stored in a –20 °C freezer. Individual scutes were catalogued by turtle ID and scute number (1 to 15, left to right, anterior to posterior) as follows: first left coastal (1), first vertebral (2), first right coastal (3), second left coastal (4), etc.

Scute samples were thawed for 24 hours prior to processing and cleaning. Barnacles and other epibiota were removed with a chisel and 80-grit sandpaper was used to remove loose keratin per SCDNR carapace preparation procedures for attaching transmitters. Scutes were rinsed with tap water and dabbed with 70% isopropyl alcohol pads prior to air drying in a fume hood. Whole scutes were subdivided into subsamples with minimum dimensions (measured with a ruler) of 3.6 cm × 3.6 cm to ensure a complete fit under a wooden mounting brace and even distribution of tensile force across the entire surface of the subsample (Figure 2.2a). As such, whole scutes <7 cm in either length or width were divided into two subsamples; whole scutes measuring <7 cm in length but >11 cm in width divided into three subsamples; and whole scutes >7 cm in length and width divided into four subsamples. From each whole scute with at least two subsamples, one subsample was randomly selected (MS Excel random number generation data tool, version 2002, Redmond, WA) for archiving.

To evaluate epoxy adhesion strength, galvanized eye-screws were mounted perpendicularly in two-component marine epoxy (Powers Pure 50+, DeWalt) to the keratinized surface of each subsample selected for testing. Epoxy surface area was calculated using circumference measured as the length of a string wrapped around the

base of the epoxy since direct measurements of radius were obscured by eye-screw placement. Epoxy mass (0.001 g precision) was deduced by subtracting the combined mass of the pre-epoxied subsample and a screw eye mass of 1.364 grams (*i.e.*, the mean of 148 screw eye masses) from fully assembled subsamples, with all measurements obtained using a Sartorius model CPA223S analytical balance. Scute (and subsample) thickness were measured (0.003 cm precision) using a dial caliper (SPI model 30-412-1).

Scute subsamples were secured to the top of a custom-built Luan plywood (0.6 cm thick) weight tray (Figure 2.2a). At one-minute intervals, dive weights (0.9 kg) were systematically added to the base of the weight tray (Figure 2.2b) up to a maximum load of 4.5 kg and a maximum trial time of 20 minutes. The maximum and mean force sustained (0.1 N precision with 0.03 N resolution) and trial duration (0.01 s precision) were measured by a PASCO (Hudson, OH) Wireless Force-Acceleration Sensor PS-3202. Data were digitally stored using proprietary SPARKvue software.

The coefficient of variation (CV) was computed to characterize the distribution of forces required to dislodge epoxy from loggerhead keratin. Cluster analysis (Minitab, version 18) was used to describe influences of the following input parameters on mean force sustained per scute subsample: turtle ID (1 to 5); scute (1 to 15); subsample position (1 to 4, left to right and top to bottom); turtle straight carapace length (SCLmin); epoxy mass (g); subsample volume (cm^3); maximum force (N); and trial duration (minutes). A two-factor ANOVA (RStudio, version 3.4.3, Boston, MA, $\alpha = 0.05$) was used to test the null hypotheses that mean maximum break force (N) was not significantly different by (a) individual sea turtle, (b) scute location on the carapace, and (c) body condition.

Objective 2 – Fatty acid analysis

Although keratin consists mostly of protein, some freshwater turtle species produce lipids that may contribute to the formation of a water-loss barrier during keratin synthesis (Alibardi & Toni, 2006a, 2006c). Therefore, to test the null hypothesis of no difference in keratin composition across individual turtles, the fatty acid profiles (FAP) of scute subsamples archived in Objective 1 were generated using gas chromatography with flame ionization detection (GC-FID). Scute subsamples were cryo-milled for pulverization and homogenization. Lipids were extracted from scutes and quality control materials using a modified Bligh-Dyer extraction with recorded sample weights and internal standards spiked prior to extraction (Bligh & Dyer, 1959; Ostermann *et al.*, 2014). Lipids were converted to fatty acid methyl esters (FAMEs) via an acid-catalyzed hydrolysis and derivatization with methyl acetate to make them amenable to gas chromatography (Lepage & Roy, 1986; Ostermann *et al.*, 2014). Extraction and derivatization steps followed procedures detailed in Appendix A.

Individual peaks in each chromatogram reflected retention time and were compared to retention times for standards using ChemStation (Version 3.02, Agilent, Santa Clara, CA). Calculations for response factors and percentages for fatty acids and total fat followed previously reported methods (AOAC, 2002). For this study, fatty acids were categorized by chain length, with short chains considered <14 carbons and long chains considered ≥14 carbons in length. Following common practices detailed by van den Berg *et al.* (2006), missing values were replaced by small-value imputation, which is equivalent to half of the minimum positive value in the entire data array. Data were scaled using the Pareto method, which centers the values about their mean and then divides each value by the square root of the standard deviation for a feature.

Principal components analyses (PCA) were performed using MetaboAnalyst (version 4.0; Chong *et al.*, 2018) to compare percentages of fatty acids across individual turtles. Student's t-tests (MS Excel, version 2002, $\alpha = 0.05$) were used to confirm separation in the first two principal components (PC1, PC2) between individual turtles. To identify fatty acids driving separation in principal components, PCA loadings were analyzed following previously reported methods (Worley & Powers, 2012). A single-factor ANOVA (MetaboAnalyst, version 4.0, $\alpha = 0.05$) was used to test for significant differences in percentages of individual fatty acids by turtle; subsequently, a Tukey HSD post hoc test was performed to determine which groups significantly differed. A Bonferroni correction was applied to adjust p-values. All regression analyses were performed using MS Excel (version 2002, $\alpha = 0.05$). Regression analysis was used to evaluate the relationship between total fat percentage of each scute subsample ($n = 64$) and mean break force (N) across all other subsamples for the 'parent' scute obtained in Objective 1. Individual fatty acid regressions were also assessed with respect to (a) mean break force across individual sea turtles, (b) mean break force pooled by body condition, and (c) mean break force pooled by scute locations on the carapace.

2.3. RESULTS

Objective 1

Carapace scutes were obtained from five loggerhead sea turtles (mean SCLmin = 65.0 cm, CV = 0.2; Table 1.2) that stranded between 7 June and 3 September 2018. Stranded loggerheads had body condition scores of 0 ($n = 2$), 1 ($n = 2$), and 2 ($n = 1$). Seventeen percent of proposed carapace scutes ($n = 13$) were unable to be collected due to physical damage from interactions with watercraft that led to the demise of the turtles.

Sixty-two carapace scutes were removed and partitioned into four (33 scutes), three (15 scutes), or two (14 scutes) subsamples, of which 143 were tested for adhesion (Objective 1) and 64 were archived for chemical analysis (Objective 2).

Mass and surface area of epoxy attachments were highly consistent among trials with a mean mass of 1.5 g (CV = 0.2) and mean surface area of 4.0 cm^2 (CV = 0.1). Trial duration (n = 143) was highly variable and ranged from instantaneous (<1 min) separation (n = 4) to no separation after 20 min (n = 29). Across the remaining 110 trials, mean trial duration was six minutes (CV = 1.2; Table 1.2) with a mean break force of 19 N (CV = 0.6) and a mean maximum force of 31 N (CV = 0.4; Figure 2.3). Mean maximum break force significantly differed among individual turtles ($P < 0.001$, df = 2) and body conditions ($P < 0.01$, df = 2), but not among scute locations on the carapace.

Cluster analysis (Figure 2.4) revealed allometric relationships between scute and subsample width (93% similarity) and length (86% similarity), as well as between these scute properties and turtle size (72% similarity). Mean scute length was 17.3 cm (CV = 0.4), and mean subsample length was 9.4 cm (CV = 0.3). Mean scute width was 11.9 cm (CV = 0.3), and mean subsample width was 5.9 cm (CV = 0.2). Scute and subsample thickness varied across trials with a mean scute thickness of 0.1 cm (CV = 0.5) and mean subsample thickness of 0.1 cm (CV = 0.5; Table 2.2). Cluster analysis revealed that scute and subsample thickness were highly correlated (91% similarity); however, these metrics were independent of other scute properties (scute and subsample length and width) and only weakly associated with trial duration and adhesion strength (54% similarity).

Objective 2

Forty-three fatty acids were identified from 64 scute subsamples. Scute total fat content was low across individual turtles (mean = 0.16%, maximum = 0.42%; Table 2.3). Significant differences in the relative occurrence of 26 fatty acids between at least two sea turtles were detected ($P < 0.05$; Table 2.3). The first two principal components (PC1, PC2) explained 54% of variance in scute material FAPs. The greatest separation in FAPs occurred along PC1 between individuals (Figure 2.6). Drivers of separation along PC1 consisted of both saturated and unsaturated fatty acids and were predominantly relatively long chain fatty acids (Table 2.4). Despite visual overlap of 95% confidence lobes, Student's t-tests confirmed separation ($P < 0.05$) in at least one principal component between all individuals. Principal component analysis (PCA) also revealed separation of standard reference materials and scute subsamples along PC1, with reference materials grouping more tightly than scute material (Figure 2.5). Pooled samples did not strongly separate from individual experimental samples along either PC1 or PC2 (Figure 2.5).

Mean epoxy break force (range = 24.0 to 38.7) was inversely related ($P = 0.02$, $r = -0.93$) with the percentage of palmitoleic acid (range = 2.9 to 4.5; Figure 2.7). Percentage of palmitoleic acid was significantly different among individuals ($P < 0.001$, $df = 4$). Percentage of erucic acid (range = 0.98 to 1.03) was significantly related to mean break force (range = 29.4 to 38.7) across body conditions ($P = 0.02$, $r = 1.00$; Figure 2.8). However, erucic acid percentage did not significantly differ among body conditions. Mean break force (N) across subsamples was not correlated with total fat percentage for corresponding scutes ($n = 61$, $r = -0.4$; Figure 2.9). Mean break force was not related to mean total fat percentage across body condition scores. Significant correlations with mean break force across scute locations on the carapace were not detected.

2.4. DISCUSSION

To obtain accurate location data, transmitters must remain attached to animals for as long as possible. Track durations may be improved by understanding the adhesion qualities of epoxies used to attach satellite transmitters. In the present study, epoxy adhesion to loggerhead keratin was highly variable across individuals and scute locations on the carapace. Although only weakly associated, scute thickness was the scute attribute most closely related to epoxy adhesion strength. Weak association may stem from high variability in scute thickness within a single scute (*i.e.*, scute thickness is a function of position on the scute). Variability in scute thickness within a single scute was also recently reported for loggerhead sea turtles by López-Castro *et al.* (2014). Since epoxy adhesion was highly variable and weakly associated with scute attributes, the present study was unable to identify a reliable predictor for epoxy detachment from loggerhead keratin. However, epoxy adhesion cannot be ruled out as a possible reason for transmission failure for shorter track durations associated with loggerhead sea turtles.

A limitation of the current study is that measurements of trial duration and associated maximum adhesion strength were underestimated for scute subsamples where no detachment occurred. Trial duration was highly variable in the current study, which is likely explained by variability observed in epoxy adhesion strength. Twenty percent of all scute subsamples failed to detach from epoxy at the maximum trial duration and maximum force sustained. This suggests the overall mean maximum epoxy adhesion strength for loggerhead scute subsamples was likely underestimated in this study. Future studies should consider further testing with additional weights to capture a broader range of maximum epoxy adhesion strength to loggerhead keratin.

Despite weak association between epoxy adhesion and scute attributes, allometric relationships were discovered between scute dimensions and turtle size, indicating that scutes grow proportionally in length and width to the size (SCLmin) of the turtle. This finding was expected given a previous observation that scute growth occurs along scute edges in hawksbill sea turtles (Palaniappan, 2007), though locations of scute growth in loggerheads remain largely unstudied. Recent literature supports allometric growth in loggerhead sea turtle carapaces. Casale *et al.* (2017) reported allometric variation in carapace shape for loggerhead hatchlings using geometric morphometrics. Additionally, allometric relationships among carapace morphometrics were documented in both green (*Chelonia mydas*) and loggerhead hatchlings (Salmon & Scholl, 2014). For loggerhead sea turtles, allometric relationships between scute thickness and turtle size (SCLmin) were not expected given the older top layers of scutes slough while newer layers are deposited underneath (Day *et al.*, 2005; López-Castro *et al.*, 2014).

Research is limited on scute growth, rate of scute deposition, and rate of scute sloughing for hard-shelled sea turtle species; however, such rates may be important to consider when attaching transmitters. Scutes grow continuously throughout the lives of hard-shelled sea turtles (López-Castro *et al.*, 2014). Thickening and hardening of keratin layers continues with age for loggerhead and green sea turtles (Solomon *et al.*, 1986) as well as for hawksbill (*Eretmochelys imbricata*) sea turtles (Palaniappan, 2007). Keratin growth and sloughing rates are unknown for loggerhead sea turtles, but the presence of commensal barnacles on scutes suggests this process may encompass several years (Day *et al.*, 2005). The rate of deposition of new scute tissue has been previously estimated for loggerhead nesting females (Vander Zanden *et al.*, 2010), but has yet to be determined

empirically and is not known for all size classes of loggerheads (López-Castro *et al.*, 2014). Loggerheads have been observed to periodically shed a whole scute or superficial layers of keratin (Day *et al.*, 2005), but the rate at which these keratin layers slough is largely undetermined for hard-shelled sea turtles (López-Castro *et al.*, 2014). Keratin sloughing conceivably impacts transmitter adhesion given that transmitters adhered to loosened keratin are susceptible to detachment. Understanding the rates of sloughing for hard-shelled sea turtles may better inform researchers as to optimal timeframes to apply transmitters to minimize risk of premature detachment.

The present study provides the first documentation of epoxy adhesion strength on the keratinous scutes of sea turtles in general, as well as the first documentation of fatty acids present in the carapacial scutes of loggerhead sea turtles. Previous studies have investigated the fatty acid composition of other sea turtle tissues, such as liver and adipose from loggerheads (Guitart *et al.*, 1999; Davidson *et al.*, 2014), plastron tissue from a leatherback (Ackman *et al.*, 1972), and adipose from green sea turtles (Joseph *et al.*, 1985; Seaborn *et al.*, 2005). Similar families of fatty acids were present in scutes in the current study when compared to liver and adipose tissues from previous studies (Guitart *et al.*, 1999; Davidson *et al.*, 2014); however, concentrations of fatty acids were lower in scutes than those observed in liver and adipose tissues. Lower concentrations of fatty acids in scutes compared to liver and adipose were expected given that scutes consist mostly of keratin proteins (Alibardi & Toni, 2006a; Wang *et al.*, 2016).

A limitation of the present study is that fatty acids residing on the outermost layers of keratin potentially degraded given that the scute removal process involved air-drying carapaces and fatty acid saturation is sensitive to changes in temperature (Marr &

Ingraham, 1962; Théberge *et al.*, 1996; Jagdale & Gordon, 1997). In comparison, fatty acids within the inner layers of keratin may have been relatively intact since Day *et al.* (2005) suggests loggerhead sea turtle scutes are fairly robust to degradation and stable for mercury content analysis. The current study was unable to validate the location of fatty acids within loggerhead keratin as scute subsamples were pulverized and homogenized during sample processing. Depending on the location of fatty acids within loggerhead keratin, one of two possible interpretations may be drawn: (a) fatty acids from the outermost layers of keratin may indicate the presence of algae, or (b) fatty acids from the inner layers of keratin may play roles in cellular membrane function.

Assuming fatty acids were intact in the outermost layers of keratin, the presence of palmitoleic acid may indicate the presence of residual algae despite scute cleaning procedures given that increasing percentages of palmitoleic acid were associated with decreasing mean break forces across individuals. Palmitoleic acid is associated with some strains of cyanobacteria (Matsunaga *et al.*, 1995) as well as species of brown and red algae (Polat & Ozogul, 2008; Bakar *et al.*, 2017). Matsunaga *et al.* (1995) reported that palmitoleic acid comprised over 50% of the total fatty acid content for *Phormidium* sp. NKBG 041105 and *Oscillatoria* sp. NKBG 091600. The presence of palmitoleic acid in the outermost (vs. innermost) keratin layers is a relatively low probability given carapace preparation procedures and subsequent heat exposure (Marr & Ingraham, 1962; Théberge *et al.*, 1996; Jagdale & Gordon, 1997); however, further investigation is recommended.

Conversely, if fatty acids were intact within the inner layers of loggerhead keratin, data presented in this study suggest that specific fatty acids may play a role in the formation of a water-loss barrier. Several fatty acids driving separation in overall FAPs of

loggerhead sea turtle keratin, notably oleic acid and arachidic acid, play important roles in cellular membrane function (Gonçalves-de-Albuquerque *et al.*, 2016). Oleic acid influences membrane fluidity, facilitates trans-membrane signaling, and remains highly stable to oxidation (Gonçalves-de-Albuquerque *et al.*, 2016; Hernandez, 2016). In humans, oleic acid serves as a key substrate for the formation of membrane components such as phospholipids, triacylglycerols, cholesterol, and wax esters (Mauvoisin & Mounier, 2011; Gonçalves-de-Albuquerque *et al.*, 2016). One possible explanation for the presence of oleic acid in loggerhead keratin is that it may serve a similar function in forming membranes components; however, the role of oleic acid in keratin of hard-shelled sea turtles is largely unknown and further study is needed.

Arachidic acid may play a role in limiting water-loss in the keratin of hard-shelled sea turtles. A previous study investigated the role of 18-methyleicosanoic acid (MEA), which is arachidic acid substituted by a methyl group at position 18 (McMullen & Kelty, 2007), in the keratin hair fibers of mammals (Jones & Rivett, 1997). MEA was predominantly associated with forming a continuous hydrophobic layer on the upper surface and edges of hair cuticle cells (Jones & Rivett, 1997). Similarity in fatty acid structure suggests that comparable to MEA in mammalian keratin, arachidic acid in sea turtle keratin may play a role in the formation of water-loss barrier. The possibility remains that such hydrophobic fatty acids potentially interact with epoxy bond strength to the carapace, subsequently influencing transmitter adhesion. Further study is warranted to empirically determine the role of arachidic acid in epoxy adhesion to hard-shelled sea turtle keratin. The presence of fatty acids in the inner layers of loggerhead keratin is more

likely since fatty acids may have been relatively protected from heat exposure given the high stability of keratin (Day *et al.*, 2005; Wang *et al.*, 2016).

Previous studies on avian and reptilian keratin suggest keratin scutes of hard-shelled sea turtles are robust to degradation. The keratinous feathers of seabirds showed that UV radiation, heating, freezing, and weathering for eight months has less than a 10% effect on mercury concentrations (Appelquist *et al.*, 1984). In addition, Moyer *et al.* (2016) demonstrated that feather keratin was extremely durable and maintained structural and microstructural integrity when subjected to different burial environments for a duration of approximately 10 years. The carapace of hard-shelled freshwater turtles consists almost entirely of β-keratin proteins, which are insoluble, filament-forming proteins with a high sulfur content (Alibardi & Thompson, 1999; Alibardi & Toni, 2006a; Wang *et al.*, 2016). Chelonian beta-keratins consist of high amounts of cysteine (Dalla Valle *et al.*, 2009), a sulfur-containing amino acid, that readily forms disulfide bonds, conferring rigidity and providing enhanced resistance to degradation (Riffel *et al.*, 2003; Moyer *et al.*, 2016). Keratinous materials are typically unreactive to the natural environment due to their high content of cysteine that distinguishes them from other proteins (Wang *et al.*, 2016). Therefore, fatty acids in the inner layers of loggerhead keratin may have been relatively intact despite heat exposure. More research is needed since studies validating the location of fatty acids within keratin scute layers of hard-shelled sea turtles have not yet been conducted.

Epoxy break force was positively associated with erucic acid percentage across declining body conditions, potentially corroborating the suggestion by Day *et al.* (2005) that scute properties are robust to degradation. This finding may explain the relatively

strong adhesion of epoxy to loggerhead keratin despite moderate decomposition. Although percentage of erucic acid did not significantly differ among body conditions, a possible explanation may be that differences were unable to be detected given the modest sample size of individuals and low amounts of erucic acid detected. Erucic acid has been studied predominantly in dietary studies (Velioglu *et al.*, 2017; Kok *et al.*, 2018; Vetter *et al.*, 2020). Although the damaging effects of erucic acid on mammalian hearts is well known (Houtsmuller *et al.*, 1970; Bozcali *et al.*, 2009; Shi & Dumont, 2014), the role of erucic acid in keratin structures has not been studied. Further research is needed to examine the influence of erucic acid on epoxy adhesion to sea turtle keratin.

Future studies may benefit from developing alternative methods of scute removal to eliminate the need for air-drying carapaces and limit the potential for fatty acid degradation in the outer layers of keratin. Preliminary methods of scute collection on frozen carcasses in the present study were aimed at limiting fatty acid degradation but ultimately were unsuccessful in removing whole, intact scutes that were free of underlying vascular tissue. Alternative methods of sample collection targeting lipids in the outermost layer of keratin, which may be in contact with epoxy, may prove useful for further chemical analyses. Future studies should also consider sampling multiple sea turtle species to assess inter-species differences in epoxy adhesion to and chemical composition of keratin. Scute removal was attempted for one Kemp's ridley carapace but scutes failed to shed after approximately 150 days of air-drying, further highlighting the need to develop alternative methods of scute removal.

Understanding the physical and chemical properties of loggerhead sea turtle keratin and of epoxies used to attach satellite transmitters may lead to future

improvements in transmitter adhesion for hard-shelled sea turtles. Epoxy adhesion to loggerhead keratin was highly variable and cannot be ruled out as a reason for transmission failure for shorter track durations. In addition, the presence of fatty acids in loggerhead scutes was documented for the first time. Fatty acids that drove separation in FAPs potentially serve roles in cellular membrane function. While the present study analyzed fatty acids, future studies should consider other chemical analyses, such as proteomics, lipidomics, and/or metabolomics, to evaluate the chemical composition of sea turtle scutes and various epoxies. Such analyses may identify differences in molecular structure that may contribute to reduced adhesion between two-component marine epoxy and hard-shelled sea turtle keratin. Identifying reasons underlying reduced adhesion of epoxy to sea turtle keratin may ultimately aid efforts to extend tracking periods for loggerheads among other hard-shelled sea turtle species in future telemetry studies.

FIGURES

Figure 2.1. Metal drying cage located at Fort Johnson. Cage measures 173 (length) cm × 61 (width) cm × 61 (height) cm. A maximum of two carcasses may be placed on either tray for air-drying to induce scute detachment.

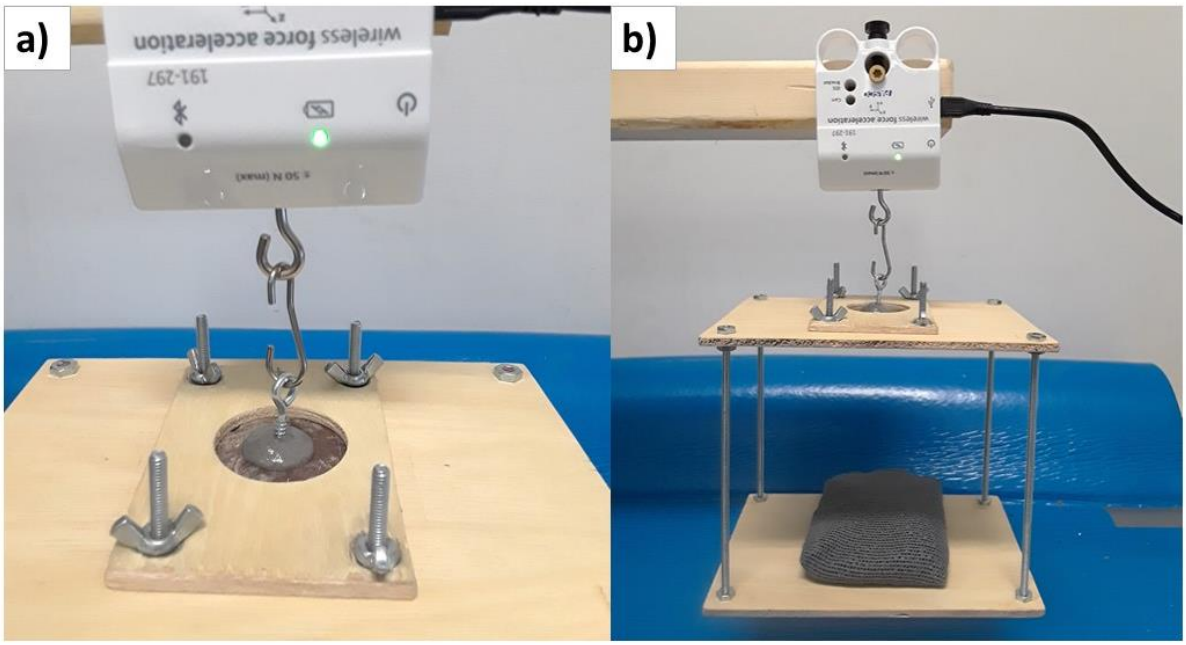

Figure 2.2. a) Top view of scute subsample with an eye-screw set in epoxy suspended from a force transducer via wooden brace with a circular cut-out measuring 3.6 cm in diameter, b) Front view of experimental apparatus with one 0.9-kg dive weight loaded onto bottom weight tray.

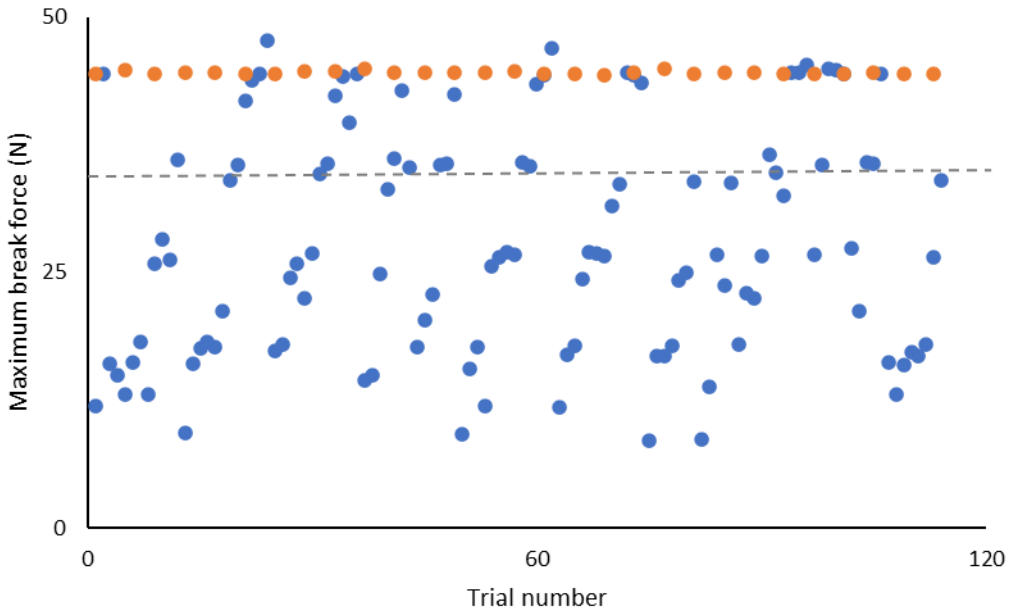

Figure 2.3. Distribution of maximum break forces (y-axis) for epoxy on loggerhead sea turtle scutes (n = 143) for epoxy detachments (blue; n = 114) and no epoxy detachments (orange; n = 29). Dashed line represents mean maximum break force across all samples.

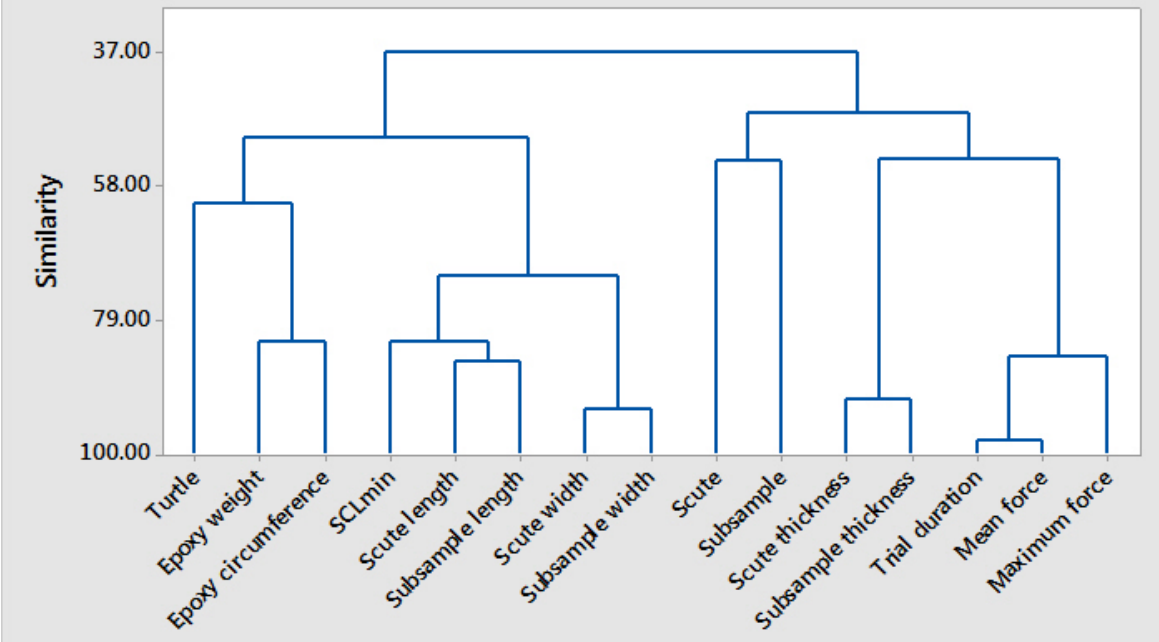

Figure 2.4. Cluster analysis (single linkage, Euclidean distance) assessing percent similarity (y-axis) between mean epoxy adhesion force, morphometric measures, and other attributes of scute subsamples (x-axis).

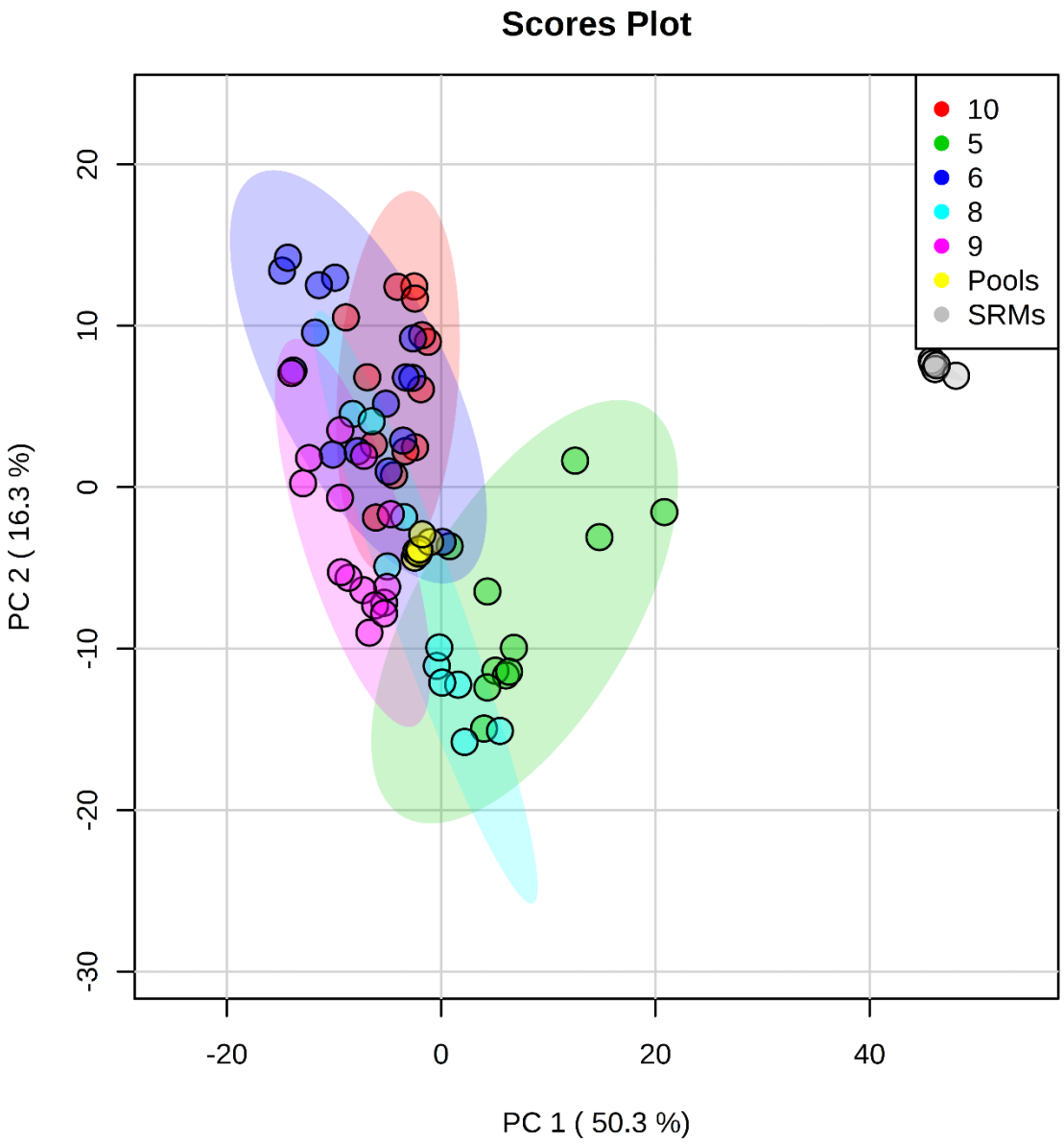

Figure 2.5. Plot of PCA scores for PC1 (x-axis) and PC2 (y-axis) for FAPs of quality control materials and loggerhead sea turtle scutes (n = 64) for five individual turtles (5, 6, 8, 9, and 10), all samples pooled (Pools), and standard reference materials (SRMs). Ellipses indicate 95% confidence regions for each group.

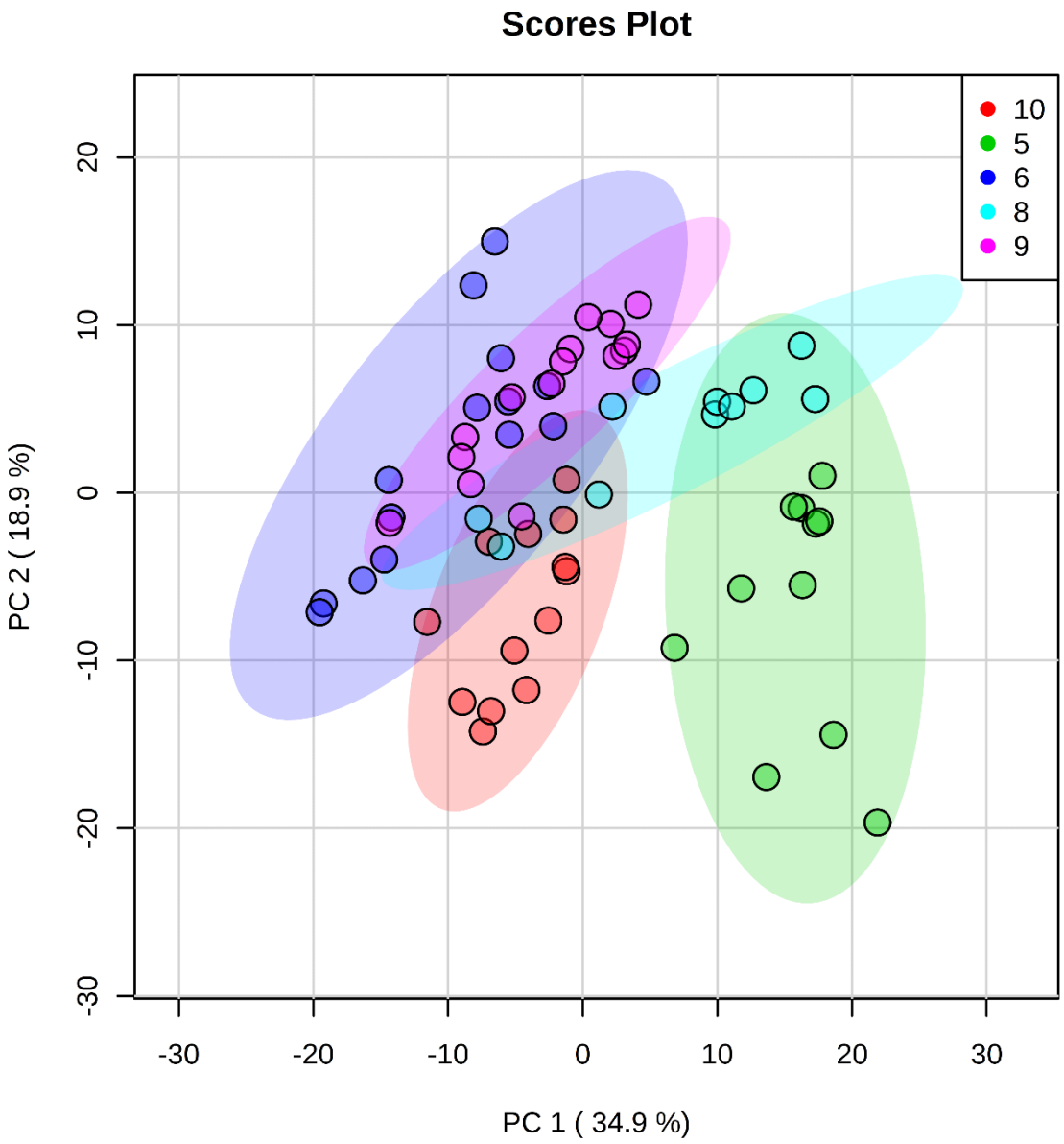

Figure 2.6. Plot of PCA scores for PC1 (x-axis) and PC2 (y-axis) for FAPs of loggerhead sea turtle scutes (n = 64) for five individual turtles (5, 6, 8, 9, and 10). Ellipses indicate 95% confidence regions for each group. Despite visual overlap of 95% confidence lobes, Student's t-tests confirmed separation ($P < 0.05$) between all individual turtles.

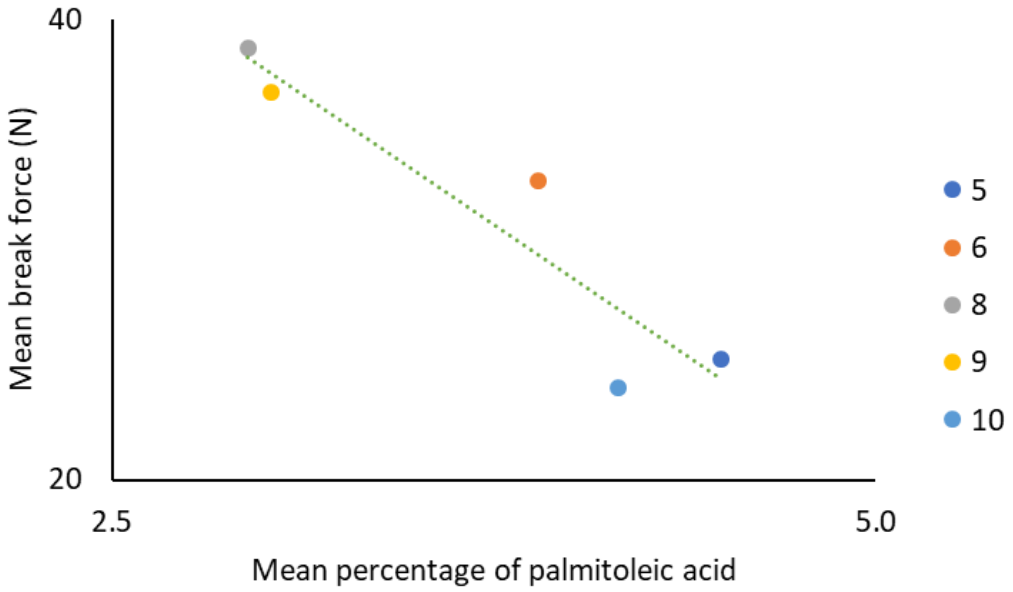

Figure 2.7. Mean break force (y-axis) vs. mean percentage of palmitoleic acid (x-axis) across individual turtles (dark blue = individual 5, orange = individual 6, gray = individual 8, yellow = individual 9, light blue = individual 10). Green dashed line represents linear trendline (r = -0.93) across all individuals.

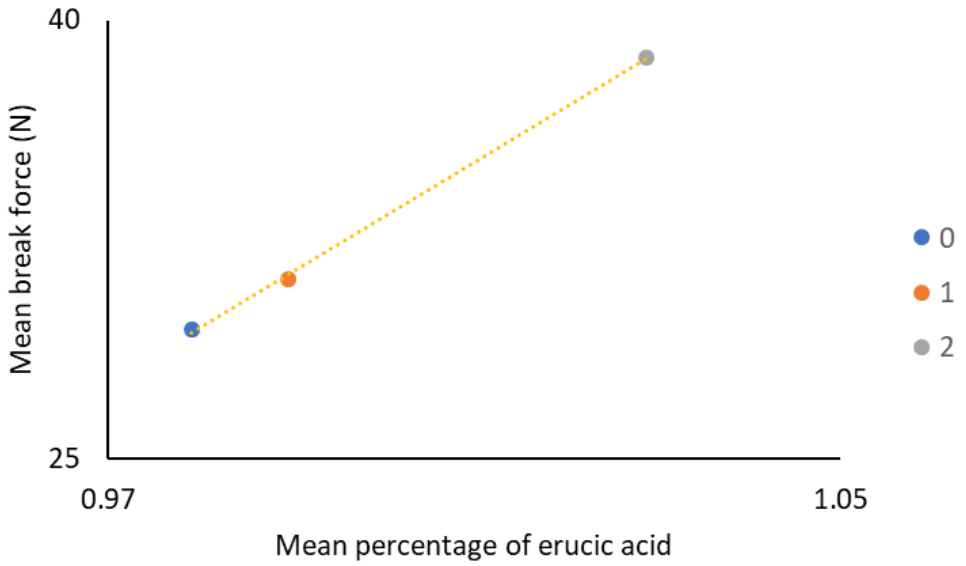

Figure 2.8. Mean break forces (y-axis) vs. mean percentage of erucic acid (x-axis) across body conditions (dark blue = body condition 0, orange = body condition 1, gray = body condition 2). Yellow dashed line represents linear trendline (r = 1.00) across all body conditions.

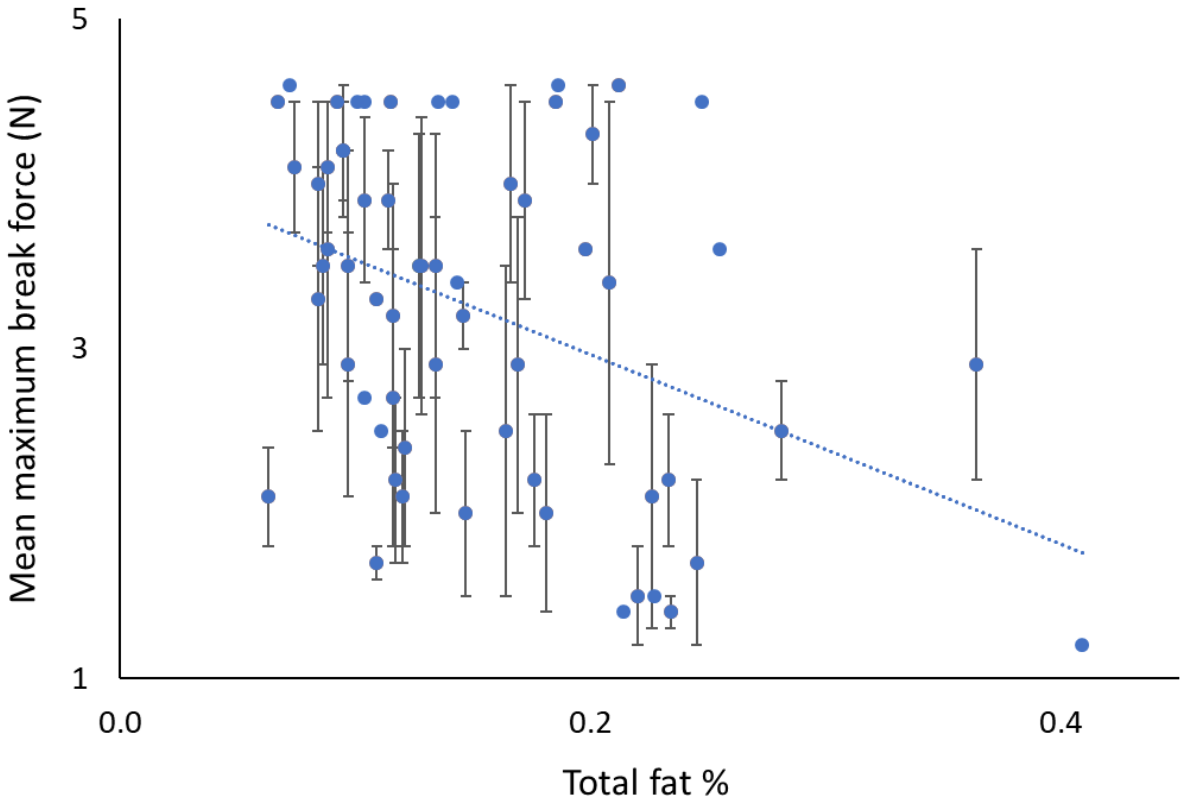

Figure 2.9. Total fat percentage (x-axis) of scute samples vs. mean (across all subsamples) break force (y-axis) for each corresponding scute tested in Objective 1 (*n* = 61). Error bars are standard error. Points with no error bars correspond to scutes with only one subsample or low (< 0.1) standard error. Blue dashed line represents linear trendline (r = -0.4) across all subsamples.

TABLES

Table 2.1. Comparison of satellite track durations among species of hard-shelled sea turtles from several recent studies using similar attachment methods.

Species	Mean (days)	SD (d)	Range (d)	Ocean basin	Source
C. caretta	163.7	103.5	29–401	NW Atlantic	(Arendt, Segars, Byrd, Boynton, Whitaker, *et al.*, 2012)
C. caretta	216	320	7–1415	NW Atlantic	(Mansfield *et al.*, 2009)
C. caretta	372	210	19–997	NW Atlantic	(Griffin *et al.*, 2013)
Mean for C. caretta	251				
L. kempii	119.5	97.0	22–506	Gulf of Mexico	(Coleman, *et al.*, 2017)
L. kempii (subadults)	46	24	11–106	Gulf of Mexico	(Seney & Landry, 2011)
L. kempii (adults)	108	88	20–277	Gulf of Mexico	(Seney & Landry, 2011)
L. kempii	109.0	29.3	8–146	Gulf of Mexico	(Shaver *et al.*, 2017)
Mean for L. kempii	96				
L. olivacea	113	81	14–297	SW Atlantic	(Da Silva *et al.*, 2011)
L. olivacea	236	142	6–779	NE Pacific	(Plotkin, 2010)
Mean for L. olivacea	175				
C. mydas	178	104	47–310	Arabian Gulf	(Robinson *et al.*, 2017)
C. mydas	80	60	1–197	SW Atlantic	(Godley *et al.*, 2003)
Mean for C. mydas	129				
E. imbricata	334	279	15–804	SW Atlantic	(Marcovaldi *et al.*, 2012)
E. imbricata	558	439	11–1302	NW Atlantic	(Hawkes *et al.*, 2012)
Mean for E. imbricata	446				

Table 2.2. Descriptive statistics for cluster analysis input variables for scutes taken from five individual loggerheads; measurements (length, width, thickness) in cm, mass in g, surface area in cm^2, duration in min, and force in N. SCLmin represents minimum straight-line carapace length; SD represents standard deviation; CV represents coefficient of variation.

	SCLmin	Scute length	Scute width	Scute thickness	Subsample length	Subsample width	Subsample thickness	Epoxy mass	Epoxy surface area	Trial duration	Maximum force	Mean force
Mean	65.0	17.3	11.9	0.0	9.4	5.9	0.0	1.5	4.0	6	31	19
SD	13.9	6.5	3.1	0.0	2.9	1.2	0.0	0.4	0.6	7	12	12
Min	50.0	7.1	6.0	0.0	5.0	3.6	0.0	0.5	2.7	0	9	1
Max	87.0	33.5	22.8	0.1	18.0	9.3	0.1	2.9	5.7	20	48	40
CV	0.2	0.4	0.3	0.5	0.3	0.2	0.5	0.2	0.1	1.2	0.4	0.6

Table 2.3. Fatty acid percentages (as FAMEs) for loggerhead sea turtle individuals (5, 6, 8, 9, and 10). Errors are standard deviation. For each fatty acid, letters indicate significant differences between pairs of individual turtles (*i.e.*, individual 5 is significantly different from individual 10 for C14:0).

Fatty acid	5	6	8	9	10
C14:0	6.03 ± 0.9[a]	7.40 ± 1[b,e,f]	5.36 ± 2[c,e]	5.94 ± 2[d,f]	8.92 ± 1[a,b,c,d]
C14:1-c9	0.855 ± 0.3[a,b]	0.269 ± 0.1[c,d]	2.17 ± 1[a,c]	3.45 ± 1[b,d,e]	1.11 ± 1[f]
C15:0	0.469 ± 0.07[a]	0.572 ± 0.1[b]	0.434 ± 0.1[b,c]	0.614 ± 0.1[a,c]	0.553 ± 0.1
C15:1-c10	n.d.	n.d.	n.d.	n.d.	0.034 ± 0.0
C16:0	14.5 ± 2[a,b]	19.3 ± 3.9[a,c,d]	16.5 ± 0.9[d]	17.1 ± 1[b]	16.3 ± 0.9[c]
C16:1-t9	0.352 ± 0.03[a]	0.458 ± 0.1[b]	0.551 ± 0.04[c]	0.743 ± 0.3[a,b,c,d]	0.418 ± 0.1[d]
C16:1-c9	4.49 ± 1[a,b]	3.85 ± 1	2.94 ± 0.5[a,c]	3.02 ± 0.5[b,d]	4.10 ± 1[c,d]
C17:0	0.923 ± 0.08[a,b]	0.705 ± 0.1[a,c]	0.868 ± 0.2[d]	0.941 ± 0.2[c,e]	0.659 ± 0.1[b,d,e]
C17:1-c10	n.d.	n.d.	n.d.	n.d.	n.d.
C18:0	13.1 ± 2[a]	11.1 ± 2[b,c]	13.8 ± 3[b,d]	13.5 ± 0.2[c,e]	9.66 ± 2[a,d,e]
C18:1-t9	0.295 ± 0.1	0.400 ± 0.2	0.507 ± 0.2	0.298 ± 0.1	0.332 ± 0.1
C18:1-t11	0.309 ± 0.2[a,b]	0.359 ± 0.2[c,d]	0.437 ± 0.2[e]	0.858 ± 0.2[a,c,e,f]	0.556 ± 0.2[b,d,f]
C18:1-c6	0.153 ± 0.05	0.153 ± 0.1	0.704 ± 0.6	0.193 ± 0.1	0.185 ± 0.2
C18:1-c9	14.3 ± 2[a,b,c]	7.84 ± 2[a,d,e]	15.2 ± 2[d,f,g]	9.50 ± 1[b,f]	11.2 ± 2[c,e,g]
C18:1-c11	3.51 ± 0.3	3.56 ± 0.8	3.87 ± 0.4	3.87 ± 0.5	3.66 ± 0.4
C19:0	0.589 ± 0.2[a,b]	0.539 ± 0.1[c]	0.412 ± 0.1[a,c]	0.471 ± 0.1[b]	0.514 ± 0.1
C18:2-t9,t12	0.248 ± 0.1	0.363 ± 0.2	0.149 ± 0.1	0.143 ± 0.1	0.207 ± 0.1
C19:1-c7	0.522 ± 0.7	0.193 ± 0.1	n.d.	0.092 ± 0.02	0.355 ± 0.2
C18:2-c9,c12	1.24 ± 0.2[a]	3.56 ± 1[a,b,c,d]	1.23 ± 0.2[b]	1.49 ± 0.6[c]	0.953 ± 0.2[d]
C20:0	3.61 ± 1.2[a,b,c]	5.72 ± 1[a,d]	4.49 ± 1[d,e,f]	6.23 ± 0.6[b,e]	6.44 ± 0.7[c,f]
C18:3G-c6,c9,c12	0.394 ± 0.3	0.234 ± 0.2	0.343 ± 0.2	0.140 ± 0.1	0.175 ± 0.2
C20:1-c5	0.241 ± 0.1[a,b,c,d]	0.120 ± 0.1[a]	0.134 ± 0.01[b]	0.087 ± 0.04[c]	0.136 ± 0.1[d]
C20:1-c8	0.194 ± 0.1	0.145 ± 0.1	0.161 ± 0.03	0.193 ± 0.1	0.265 ± 0.1
C20:1-c11	1.124 ± 0.4[a,b,c]	0.605 ± 0.1[a,d]	0.771 ± 0.1[b]	0.606 ± 0.1[c,e]	1.00 ± 0.2[d,e]
C18:3-c9,c12,c15	0.505 ± 0.1[a]	1.44 ± 1[a,b,c,d]	0.439 ± 0.1[b]	0.761 ± 0.3[c]	0.634 ± 0.2[d]
C21:0	0.866 ± 0.6	1.01 ± 0.2	0.770 ± 0.2	0.902 ± 0.1	0.881 ± 0.1
C18:2-c9,c11	0.350 ± 0.2	0.355 ± 0.3	0.262 ± 0.2	0.227 ± 0.2	0.201 ± 0.1
C20:2-c11,c14	0.488 ± 0.2	0.358 ± 0.2	0.530 ± 0.2	0.348 ± 0.1	0.395 ± 0.1
C22:0	6.00 ± 1[a,b,c,d]	9.13 ± 2[a]	8.00 ± 1[b]	9.12 ± 1[c]	8.13 ± 0.6[d]
C20:3G-c8,c11,c14	0.358 ± 0.2	0.184 ± 0.1	0.285 ± 0.2	0.312 ± 0.1	0.355 ± 0.2
C22:1-t13	0.426 ± 0.3	0.165 ± 0.1	0.148 ± 0.05	0.120 ± 0.1	0.206 ± 0.1
C22:1-c13	0.902 ± 0.4	1.13 ± 0.5	1.03 ± 0.3	0.772 ± 0.2	1.29 ± 0.4
C20:3-c11,c14,c17	0.461 ± 0.2	0.675 ± 0.3	0.494 ± 0.1	0.489 ± 0.2	0.786 ± 0.3
C20:4-c5,c8,c11,c14	8.04 ± 2[a,b,c,d]	3.39 ± 0.7[a,e]	4.89 ± 0.8[b,e,f]	4.01 ± 0.4[c]	3.39 ± 0.4[d,f]
C22:2-c13,c16	0.200 ± 0.1[a]	0.485 ± 0.4[a,b,c]	0.197 ± 0.1[b]	0.162 ± 0.1[c]	0.270 ± 0.1
C24:0	2.25 ± 0.4[a,b,c,d]	4.74 ± 0.9[a,e]	3.86 ± 1[b]	4.48 ± 0.9[c,f]	3.36 ± 0.3[d,e,f]
C20:5-c5,c8,c11,c14,c17	1.02 ± 0.4[a,b,c,d]	0.233 ± 0.2[a,e]	0.387 ± 0.1[b]	0.364 ± 0.3[c]	0.485 ± 0.2[d,e]
C24:1-c15	2.94 ± 0.6[a,b,c,d]	6.24 ± 2[a]	5.10 ± 2[b]	5.15 ± 2[c]	6.73 ± 1[d]
C22:3-c13,c16,c19	n.d.	1.37 ± 0.02	n.d.	0.971 ± 0.5	1.36 ± 0.5
C22:4-c7,c10,c13,c16	1.38 ± 0.3[a]	0.982 ± 0.2[a,b]	1.18 ± 0.3[c]	1.25 ± 0.3[d]	1.66 ± 0.6[b,c,d]
C22:5-c4,c7,c10,c13,c16	1.35 ± 0.4[a,b,c]	1.18 ± 0.2[d]	0.893 ± 0.2[a]	0.876 ± 0.2[b,d]	0.945 ± 0.3[c]
C22:5-c7,c10,c13,c16,c19	1.66 ± 0.7[a,b,c,d]	0.556 ± 0.1[a,e]	0.671 ± 0.2[b,f]	0.507 ± 0.2[c,g]	1.18 ± 0.5[d,e,f,g]
C22:6-c4,c7,c10,c13,c16,c19	4.48 ± 2[a,b,c,d]	1.22 ± 0.3[a]	1.01 ± 0.3[b]	0.956 ± 0.3[c]	1.49 ± 0.6[d]
Total fat	0.141 ± 0.05[a]	0.144 ± 0.1[b]	0.100 ± 0.04[c]	0.151 ± 0.1[d]	0.252 ± 0.1[a,b,c,d]
Total saturated	0.065 ± 0.02[a]	0.086 ± 0.04[b]	0.055 ± 0.02[c]	0.093 ± 0.04[d]	0.138 ± 0.04[a,b,c,d]
Total monounsaturated	0.039 ± 0.01[a]	0.034 ± 0.02[b]	0.031 ± 0.01[c]	0.040 ± 0.01[d]	0.074 ± 0.02[a,b,c,d]
Total polyunsaturated	0.029 ± 0.01[a]	0.020 ± 0.01[b]	0.012 ± 0.00[a,c]	0.018 ± 0.01[d]	0.034 ± 0.02[b,c,d]
ω-3	0.012 ± 0.01[a]	0.005 ± 0.00[b]	0.003 ± 0.00[a,c]	0.005 ± 0.00[d]	0.014 ± 0.01[b,c,d]
ω-6	0.017 ± 0.00	0.015 ± 0.01	0.009 ± 0.00	0.013 ± 0.01	0.020 ± 0.01

Table 2.4. Absolute value of the first principal component (PC1) loadings scores for fatty acids (length of hydrocarbon chain: degree of unsaturation-configuration and location of double bonds) driving separation in overall FAPs between individual turtles.

Fatty acid	Common name	PC1
C18:1-c9	Oleic	0.47
C24:1-c15	Nervonic	0.34
C20:4-c5,c8,c11,c14	Arachidonic	0.32
C22:0	Behenic	0.31
C20:0	Arachidic	0.29
C18:0	Stearic	0.29
C24:0	Lignoceric	0.27
C14:0	Myristic	0.26
C22:6-c4,c7,c10,c13,c16,c19	DocosaHexaenoic (DHA) (ω -3)	0.22

CHAPTER 3. CHARACTERIZATION OF SCUTE SURFACE TEXTURE

3.1. INTRODUCTION

Across materials, surface texture is an important determinant of friction, and in turn, adhesion. Pavement surface roughness is critical to maintain proper levels of skid resistance on roadways (Asi, 2007). Likewise, floor surface texture relates to the potential for fall-related injuries (Grönqvist *et al.*, 2003). In ecological research, surface rugosity is often used as an indicator of biodiversity levels for benthic habitats (Luckhurst & Luckhurst, 1978; Jacobi & Langevin, 1996). Other studies have characterized the surface texture of biotic materials such as sea turtle keratin, but such studies provide mainly qualitative descriptions (Espinoza *et al.*, 2007; Palaniappan, 2007; Fuller *et al.*, 2010).

In addition to being important across fields of study, numerous methodologies exist for measuring surface texture. Metrics such as friction coefficient (Blau, 2001), resistive force (Asi, 2007), and epoxy adhesion strength (Zhai *et al.*, 2008) are widely used in industrial studies to measure different types of forces. Friction coefficients, defined as the ratio of the sliding resistance between two objects and the pressure between the two surfaces, are valuable for selecting materials and lubricants in mechanized processes (Blau, 2001). Resistive force can be measured using the British Pendulum Tester to characterize the skid resistance of various asphalt-concrete mixes (Asi, 2007), where skid resistance is a measure of shear stress. Epoxy adhesion strength, a measure of normal stress, has been used to determine how well an epoxy is able to bond

to various substrata and is measured using specialized equipment in materials science applications (Zhai *et al.*, 2008). Optical and mechanical profilometers analyze surface roughness using an optical beam that measures three-dimensional surfaces (Joniot *et al.*, 2006), while slip meters characterize surface slickness using pneumatic test wheels to simulate heel strikes (Grönqvist *et al.*, 2003). Given these instruments are designed for specialized purposes, such methods are impractical for use in this study.

In contrast to industrial applications, studies investigating the surface roughness of sea turtle carapacial scutes are limited, which is surprising given reliance on epoxy to secure data logging devices to free-swimming sea turtles. Therefore, the third objective was to characterize the surface texture of loggerhead sea turtle keratin. Surface texture characterization is a crucial precursor for identifying suitable substitute materials for testing physical factors separate from biochemical composition. Substitute carapace materials are necessary for use in controlled experiments to (a) reduce variability in substrate properties, and because (b) sea turtles are federally protected under the Endangered Species Act (ESA); as such, access to sea turtle scutes is highly regulated.

3.2. METHODS

Objective 3: Characterize the surface texture of loggerhead sea turtles and identify substitute carapace materials

Multiple techniques were used to characterize the surface texture of loggerhead sea turtles and synthetic materials, the chronological order of which is detailed below and summarized in Figure 3.1. Two laboratory metrics were used to characterize the surface texture of loggerhead sea turtle scute subsamples that remained sufficiently intact

following the completion of Objective 1. The friction coefficient was evaluated using water, a solvent, and vegetable oil; however, this metric proved unreliable and was quickly abandoned as detailed in Appendix B. Resistive force (N) of loggerhead sea turtle scutes was measured by pulling a wooden block (8.7 × 5.0 cm) across five randomly selected (MS Excel random number generator, version 2002) loggerhead sea turtle scute subsamples that were (a) larger than the block and (b) devoid of residual epoxy from Objective 1. Scute subsamples were edge-mounted to a flat, plexiglass baseplate using duct tape, then clamped to a flat surface to prevent movement during trials. The wooden block was centered on each scute subsample and pulled via an inserted eye-screw until the block began to slide across the substrate. Resistive force was measured using a PASCO sensor and proprietary SPARKvue software. Five measurements of resistive force were recorded for each scute subsample.

The resistive force was also evaluated for plexiglass (Optix, Plaskolite) and two types of ceramic tile (American Olean; hereinafter referred to as tile 1 and tile 2). Plexiglass and the two types of ceramic tile were chosen to represent a variety of surface textures. Five measurements of resistive force were measured for each of five replicates of plexiglass. Only 10 measurements for a single replicate of tile 1 and tile 2 were recorded as these were the only available tiles. Subsequent to initial testing, the substrates with the highest and lowest mean resistive forces were selected for testing additional replicates (40 total) five times each to account for variability.

Epoxy adhesion tests akin to Objective 1 were repeated with 23 materials to identify a substrate with (a) similar break force to that of loggerhead sea turtle scutes per Objective 1 and (b) a high degree of consistency among tested replicates. A minimum of

three replicates per substrate were evaluated, and testing methods resembled Objective 1. A maximum load of 44 N and a maximum trial time of 20 minutes were used for substrate testing, corresponding to peak performance for a loggerhead sea turtle scute. The coefficient of variation (CV) was computed to characterize the distribution of forces required to dislodge epoxy from various substrate types. Additional epoxy adhesion tests were performed for potentially suitable materials to increase sample size for characterizing intra-material variability as described in Appendix C. A maximum load of 620 N and a maximum trial time of 20 minutes were used for additional testing,

3.3. RESULTS

Objective 3

Mean resistive force for loggerhead sea turtle scute subsamples was 0.4 N (CV = 0.2, n = 25 observations). Relative to loggerhead scute subsamples, the highest mean resistive force was observed for plexiglass and the lowest was observed for tile 1 (Table 3.1). Subsequent testing of additional replicates revealed highly consistent resistive force for plexiglass (CV = 0.1, mean = 0.5 N, n = 200 observations) and tile 1 (CV = 0.2, mean = 0.2 N, n = 200 observations; Figure 3.2). None of 23 substrate types resembled loggerhead sea turtle scutes with respect to break force. Epoxy failed to separate from 17 substrates (74%) at a maximum sustained force of 44 N for 20 minutes. Epoxy separated from plexiglass (Optix, Plaskolite), thick plexiglass (Lexan, Plaskolite), vinyl siding (Compass, Georgia-Pacific), galvanized metal step flashing (Amerimax), vinyl end cap (Amerimax), and vinyl gutter (Amerimax; Table 3.2). For additional tests, mean maximum break force was 130 N (CV = 0.5) for 25 replicates of laminate flooring and 380 N (CV = 0.5) for 25 replicates of tile 1.

3.4. DISCUSSION

Identifying synthetic materials with surface texture similar to biotic materials is complex and requires consideration of the geometric, chemical, physical, and mechanical characteristics of the surface (Petropoulos *et al.*, 2010). The present study is the first to empirically characterize the surface of loggerhead sea turtle scute material via epoxy adhesion and resistive force tests, whereas other studies emphasized qualitative properties. Fuller *et al.* (2010) described the texture of loggerhead sea turtle scutes as "more rugose and flaky" than green sea turtle (*C. mydas*) scutes. Palaniappan (2007) documented the texture of hatchling hawksbill (*E. imbricata*) scutes as "wrinkled and rough" compared to smoother areas of new scute growth. Espinoza *et al.* (2007) also described pigmentation, patterning, and thickness of hawksbill scutes.

Substitute carapace materials identical in properties to loggerhead sea turtle keratin were not identified, but reasonable substitutes were identified for simulation experiments. Lower CVs observed in resistive force tests are likely explained by the considerably larger sample sizes relative to epoxy adhesion tests. Overall, resistive force and epoxy adhesion tests both produced consistent results, but with metric values that were dissimilar to loggerhead sea turtle scutes. These findings highlight the need to identify more realistic substrates that are comparable in surface texture to loggerhead sea turtle keratin. Characterizing surface texture remains important in understanding and improving adhesion of two-component marine epoxies to biotic media.

FIGURES

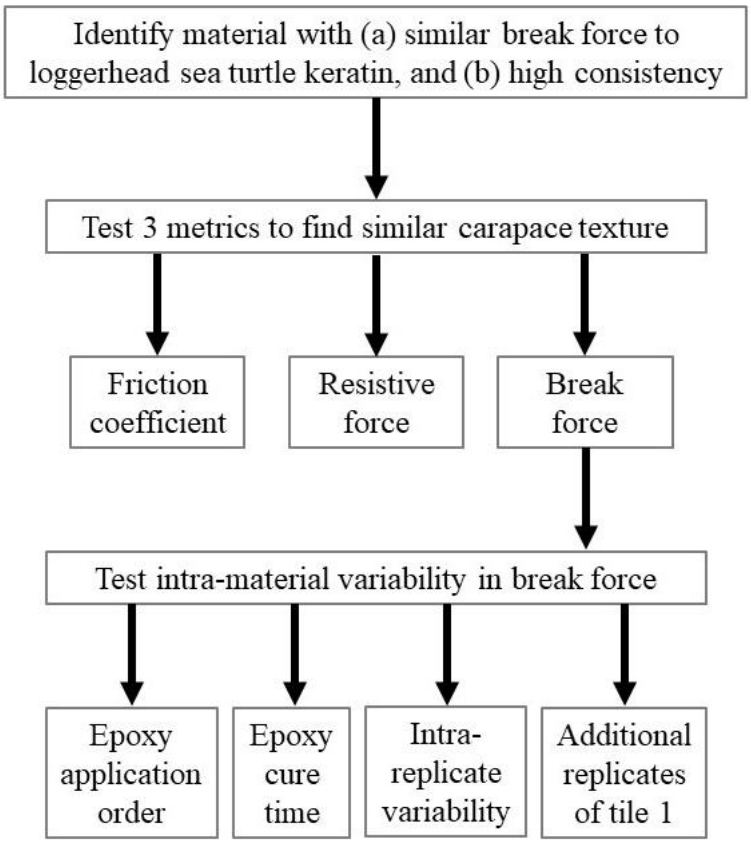

Figure 3.1. Chronological order (from top, then left to right) of techniques used to characterize loggerhead sea turtle scutes and identify proxy materials.

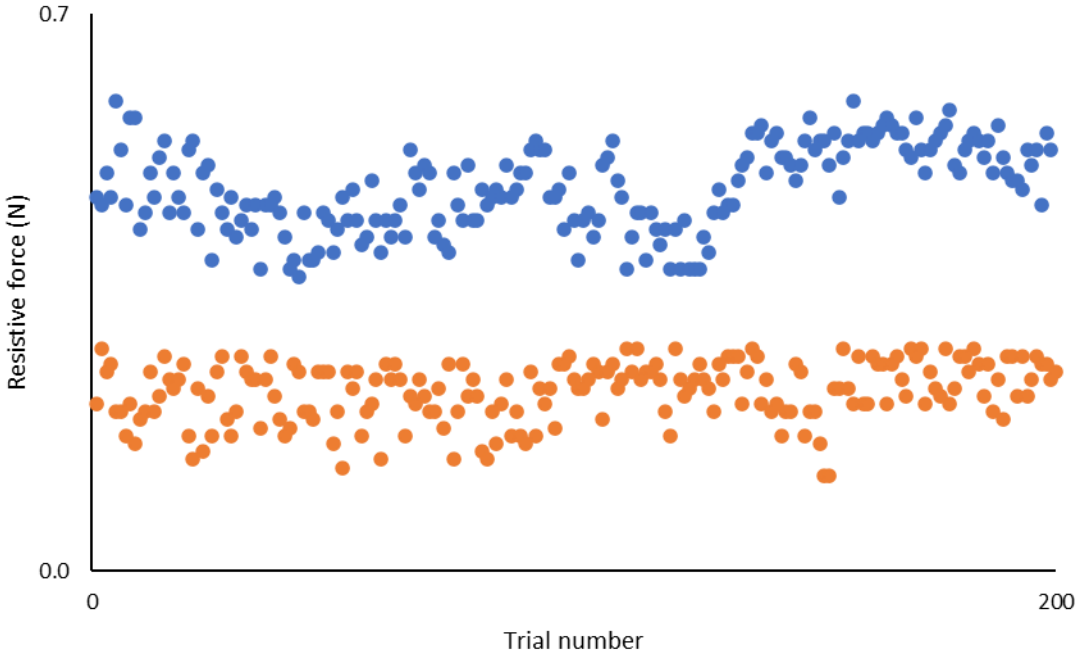

Figure 3.2. Resistive force (y-axis) for plexiglass (blue) and tile 1 (orange). Trials (x-axis) denote 40 replicates tested five times each.

TABLES

Table 3.1. Descriptive statistics for the resistive force (N) of various substrate types; CV represents coefficient of variation.

Substrate	Mean ± SD	CV	Number of replicates	Total number of observations
Scute subsamples	0.4 ± 0.1	0.2	5	25
Plexiglass	0.5 ± 0.0	0.1	5	25
Tile 1	0.2 ± 0.0	0.2	1	10
Tile 2	0.3 ± 0.0	0.1	1	10

Table 3.2. Descriptive statistics for the mean maximum break force (N) of epoxy on various substrate types; SD represents standard deviation; CV represents coefficient of variation; *n* represents number of replicates.

Substrate	Mean ± SD	CV	*n*
Plexiglass	24 ± 5.1	0.2	3
Thick plexiglass	45 ± 0.2	0.0	3
Vinyl siding	3.9 ± 1.5	0.4	3
Galvinized metal step flashing	4.8 ± 4.1	0.9	3
Vinyl end cap	38 ± 12	0.3	3
Vinyl siding	35 ± 17	0.5	3

CHAPTER 4. SURROGATE TRANSMITTER RETENTION

4.1. INTRODUCTION

Deciphering the underlying causes of satellite transmitter signal loss in telemetry records is necessary to direct future improvements in transmitter technology and attachment methods (Hays *et al.*, 2007). Additionally, understanding reasons for transmission cessation is critical in assessing the status of tracked animals (*i.e.*, alive or dead) to infer mortality rates for stock assessments (Hays *et al.*, 2003, 2007; Chaloupka *et al.*, 2004). Previous advancements in transmitter technology include transmitter miniaturization to target juvenile life stages (Hays *et al.*, 2007; Seney *et al.*, 2010; Mansfield *et al.*, 2012) and enhanced hydrodynamic design of transmitters to reduce drag and improve animal welfare (Wyneken, 1988; Watson & Granger, 1998). Despite such advancements, telemetry studies on hard-shelled sea turtles can suffer from premature transmitter detachment (Hays *et al.*, 2007; Seney, 2008; Piacenza *et al.*, 2018). In some but not all cases, causes of signal loss can be inferred using diagnostic information from satellite tags and interpreting location data prior to signal loss (Hays *et al.*, 2007).

There are numerous reasons satellite transmitters stop relaying signals, such as battery life exhaustion, saltwater switch hijacking, antenna damage, and premature detachment (Hays *et al.*, 2007; Piacenza *et al.*, 2018). Battery life on satellite tags can last for over a year (Hays *et al.*, 2006, 2007; Fujisaki *et al.*, 2016), but battery exhaustion is

rarely the cause of transmission cessation for longer successful deployments (Hays *et al.*, 2007). More often, biofouling over saltwater switches is cited as a culprit for transmission failure (Hays *et al.*, 2004, 2007; Seney, 2008; Varo-Cruz *et al.*, 2013). Physical damage to the transmitter antenna may also cause transmission failure for sea turtle species that groom against hard substrata (Caine, 1986; Watson & Granger, 1998; Hays *et al.*, 2007; Seney, 2008). Premature detachment of transmitters may result from rapid growth rates, insufficient attachment, and/or interactions with turtle excluder devices (TEDs) or watercraft (Hays *et al.*, 2007; Seney, 2008). While there has been notable effort to document reasons underlying signal loss, previous studies have often overlooked species-specific causes, such as carapace morphology.

The role of carapace morphology and epoxy footprint on retention of satellite transmitters is poorly understood for hard-shelled sea turtle species. Satellite transmitters do not always fully adhere against the curved carapaces of hard-shelled sea turtles, with some studies reporting visible gaps between the carapace and cured adhesives for animals re-examined in a captive setting after days (Mansfield *et al.*, 2012) to weeks (Seney, 2008). Seney (2008) noted gaps between the carapace and adhesives that ultimately resulted in transmitter detachment for fast-growing juvenile loggerhead sea turtles. Epoxy footprint has been briefly mentioned in previous tagging studies (Seney, 2008; McClellan & Read, 2009; Fujisaki *et al.*, 2016). However, the scientific literature is sparse regarding how carapace curvature and epoxy footprint affect transmitter retention.

While termination of signal transmission occurs for numerous reasons, the present study focuses on the role of carapace morphology and epoxy footprint on transmitter retention. The fourth objective tested the effects of simulated carapace angle (0º or 30º)

and epoxy footprint corresponding to transmitter size (small or large) on epoxy break force. For the fifth objective, a field study evaluated the effects of biofouling and submergence in seawater on surrogate transmitter retention for the aforementioned epoxy footprints and carapace angles using substitute carapace materials identified in Chapter 3. Sloan *et al.* (2014) used comparable materials to slate tile and plexiglass for field experiments conducted in Charleston, SC over several weeks; thus, given similar materials, deployment locations, and deployment durations between studies, tile 1 and laminate flooring were expected to withstand seawater submersion in Objective 5.

4.2. METHODS

Objective 4 – Epoxy footprint and carapace angle

To track movements of subadult and adult loggerhead sea turtles, SCDNR has used Telonics ST-20 and TAM-4525 satellite transmitters measuring 14.9 cm (length) × 7.4 cm (width) × 3.9 cm (height). Comparatively, Telonics TAM-4310 transmitters measuring 10.3 cm (length) × 4.6 cm (width) × 3.0 cm (height; and Iridium transmitters of similar dimensions) have been used for tracking juvenile Kemp's ridleys. The amount of epoxy associated with just the base of large transmitters attached to loggerheads was 2.3× greater than for small transmitters attached to Kemp's ridley sea turtles. Therefore, a laboratory experiment was performed to test the null hypothesis of no difference in shear force required to dislodge transmitters as a function of epoxy footprint.

Prior to epoxy application, individual substrates (tile 1) were wiped with dry paper towels to remove surface impurities, but were not sanded to smooth surface texture. Twenty small (8.7 × 5.0 cm) and 20 large (12.5 × 8.5 cm) wooden blocks that served as

surrogate transmitters were epoxied to 40 individual substrates by three researchers. For each surrogate transmitter, the two-part base epoxy used by the SCDNR (Powers Pure 50+, DeWalt) was smeared evenly on the underside (~0.6 cm deep), spread in a 4.0 cm arc around the base, and then built up 1.2 cm around the sides to simulate SCDNR attachments (Figure 4.1). The combined mass (1 g precision) of each surrogate transmitter and substrate (hereinafter referred to as experimental units) was recorded prior to and following epoxy application to quantify the amount of epoxy (g) applied. Large and small experimental units were stratified based on applied epoxy mass (107 to 214 g, 109 to 210 g for large; 51 to 139 g, 55 to 132 g for small), then randomly assigned to 0° and 30° angle treatment groups, where angle represented carapace slope (Appendix D). Surface area of the elliptical base epoxy footprint (cm^2) was calculated from measurements of footprint diameters (0.1 cm precision) since direct measurements of radii were obscured by transmitter placement.

Ten small and 10 large tile experimental units were clamped to a wooden surface with an adjustable incline (Figure 4.2) for the corresponding treatment group. During initial trials, 16 tile experimental units sustained a maximum load of 72.6 kg for 20 minutes; thus, subsequent trials began with 72.6 kg in the wooden weight tray. Additional weights (4.5 kg) were added in one-minute increments up to a maximum load of 99.8 kg and a maximum trial time of 20 minutes. The maximum force sustained (1 N precision) and duration of each trial (0.1 s precision) were recorded. A single-factor ANOVA (RStudio, version 3.4.3, Boston, MA, $\alpha = 0.05$) was used to test the null hypothesis of no difference in amount of epoxy applied by researcher for both transmitter sizes. A coefficient of variation (CV) was calculated to characterize distribution of epoxy masses.

Objective 5 – Weathering field tests

For the final objective, a field study evaluated the effect of biofouling and submergence in seawater on surrogate transmitter retention for large and small epoxy footprints (but at a 0° angle) prepared as described in Objective 4. Laminate flooring and tile 1 were selected as substitute carapace materials for use in field tests since break forces were consistent for both substrates. Surrogate transmitters first received three coats of fast-drying polyurethane clear gloss (Minwax) to prevent swelling in seawater, and were then coated with anti-fouling paint (Rust-oleum Marine Coatings Boat Bottom) in accordance with SCDNR transmitter attachment protocol.

To test the null hypothesis of no effect of *in situ* biofouling on epoxy retention across carapace angles, laminate flooring was cut into 40 replicates measuring approximately 5 cm × 9.5 cm. To prevent disintegration in water, three coats of fast-drying polyurethane clear gloss (Minwax) were applied to all laminate sides except the surface where epoxy was applied. The mass (g) of each laminate flooring replicate was recorded prior to and following epoxy application to quantify amount of epoxy (g) applied. Treatments consist of simulated carapace angles of 0º (n = 20) and 30º (n = 20). Twenty replicates per treatment (0°, 30°) was selected based on stabilization in standard error at this replicate level in previous tests with this material (Figure 4.3).

Six PVC frames were constructed to hold tile replicates and a seventh frame was built for laminate replicates as detailed in Appendix E. Frames were deployed on the seafloor by scientific SCUBA divers at the SCDNR ODMDS I4 site (32.610°N, -79.717°W) located roughly 20 km offshore in 17 m of water. This location was selected based on favorable underwater visibility for photography, live bottom habitat indicative

of biological activity, minimal interference from trawling, and relative ease of access for routine monitoring. Frames were deployed on 30 September 2019, then re-surveyed by scientific divers on 29 October (29 days) and 6 December 2019 (67 days), which exceeded the median (51 days) track duration for 23 Kemp's ridley sea turtles tagged with satellite transmitters by SCDNR between 2016 and 2019 (M. Arendt, pers. comm.).

Scientific divers video surveyed replicate frames using GoPro cameras, with at least two seconds of close-up video per replicate to ensure a clear image was obtained. Review of GoPro video occurred in a laboratory setting. Attachment/detachment was noted for each replicate. Percent epibiota cover on replicates was calculated as the aggregate cover (independent of colonizing species) on three surfaces: exposed tile or laminate flooring, epoxy, and wooden block (all three-dimensional surfaces). The three surfaces of interest were each divided into quadrats and percent cover was evaluated based on the sum of four replicate assessments.

Fisher's exact test (VassarStats, $\alpha = 0.05$) was used to determine the effect of epoxy footprint (small or large) on surrogate transmitter retention across monitor dates. In addition to descriptive statistics, Student's t-tests were used to test for differences in epoxy mass between attached and detached replicates for both transmitter sizes. A two-factor ANOVA was used to determine if epoxy mass differed by researcher and when comparing attached vs. detached replicates. Two-factor ANOVAs were used to examine differences in percent cover for small vs. large epoxy footprints across monitor dates and surfaces. For laminate flooring replicates, Fisher's exact test (VassarStats, $\alpha = 0.05$) was also used to determine the effect of simulated carapace angle (0^{o} or 30^{o}) on epoxy

retention across monitor dates. Two-factor ANOVAs were used to examine differences in percent cover for angled vs. flat replicates across monitor dates and surfaces.

4.3. RESULTS

Objective 4

Applied epoxy mass was significantly different ($P < 0.001$, $df = 1$) between small (mean = 88 g, CV = 0.3) and large (mean = 144 g, CV = 0.2) transmitters. Base epoxy footprint was 1.5 times greater for large (277 cm^2) than for small (181 cm^2) transmitters. Applied epoxy mass was also significantly different by researcher ($P < 0.001$, $df = 2$; Figure 4.4), and ranged from 51 to 139 g for small and 107 to 214 g for large transmitters. Ten small and 10 large replicates tested at no angle sustained a force of 979 N for 20 minutes, and eye-screws began to deform with additional weight. No detachments occurred for either transmitter size, and no further testing was conducted.

Objective 5

By 29 October 2019, 29 days following initial submergence, five small (25%) and two large (11%) surrogate transmitters detached from tiles. Transmitter detachments occurred only on frames 4 and 6. No epoxy detachments occurred for laminate flooring replicates. By 6 December 2019, 67 days following initial submergence, only one additional small surrogate transmitter detached from frame 4 for a study total of six small (30%) and two large surrogate transmitter detachments. No epoxy detachments occurred for laminate flooring replicates across monitor dates.

For small and large transmitter replicates 29 days following initial submergence, mean percent cover was 70% (CV = 0.5, $n = 39$) on tile, 95% (CV = 0.1, $n = 32$) on

epoxy, and absent on wooden blocks (Figure 4.5). For angle testing, mean percent cover was 90% (CV = 0.2, *n* = 40) on laminate flooring, and 85% (CV = 0.3, *n* = 40) on epoxy (Figure 4.6). For small and large transmitter replicates 67 days following initial submergence, mean percent cover was 71% (CV = 0.4, *n* = 39) on tile, 98% (CV = 0.1, *n* = 31) on epoxy, and 6% (CV = 0.8, *n* = 31) on wooden blocks (Figure 4.5). Mean percent cover on angled replicates was 91% (CV = 0.1, *n* = 40) on laminate flooring and 87% (CV = 0.3, *n* = 40) on epoxy (Figure 4.6).

Small transmitter detachment did not reflect epoxy mass, which did significantly differ among researchers ($P < 0.005$, df = 2). Three of six small transmitters that detached were applied by researcher 1, two were from researcher 2, and one was from researcher 3. Researchers 1 and 3 each attached a large transmitter that detached post-submergence. Small transmitters detached from every position within tables (2, 4, 6, and 7), and large transmitters detached from positions 1 and 6 (Figure AE.1). Fisher's exact test revealed detachment was not significantly different by transmitter size ($P = 0.24$). Overall percent cover on tile replicates was significantly different by surface ($P < 0.001$, df = 2), but not between monitor dates ($P = 0.32$, df = 1; Figure 4.5). Wooden block was the only surface to significantly increase in percent cover ($P < 0.001$, df = 1) from monitor date 1 (range = 0%) to monitor date 2 (range = 0% to 12.5%).

Given no detachments occurred for laminate flooring replicates, no statistical analysis on epoxy retention by simulated carapace angle or monitor date was performed. Percent cover on laminate flooring was significantly affected by the interaction of angle and monitor date ($P < 0.05$, df = 1), but not by angle or monitor date alone. Similarly, percent cover on epoxy was significantly affected by the interaction of angle and monitor

date ($P < 0.001$, $df = 1$), but not by angle or monitor date. Overall, no significant differences in percent cover were detected between surfaces or monitor dates.

4.4. DISCUSSION

Adhesives play an important role in a wide range of applications including construction, dentistry, and satellite telemetry. For telemetry studies on hard-shelled sea turtles, adhesives must withstand hydrodynamic forces exerted on the transmitter as an animal swims in addition to forces caused by external factors (*i.e.*, grooming against hard substrata; Watson & Granger, 1998; Seney *et al.*, 2010). Previous research on the hydrodynamic effects of transmitters on hard-shelled sea turtles has focused more on swimming behavior and energetics (Watson & Granger, 1998; Jones *et al.*, 2013) rather than adhesive properties, though Mansfield *et al.* (2012) evaluated tag attachment methods using novel adhesive combinations. While previous studies have provided qualitative descriptions of the properties of epoxy used to attach transmitters (Mitchell, 2000), few studies have empirically tested the mechanical and physical properties of adhesives in the context of attaching transmitters to hard-shelled sea turtles.

The amount of epoxy used to attach full-sized transmitters to substitute carapace materials was quantified in the present study. Predictably, large transmitters received significantly more epoxy than small transmitters. The amount of epoxy applied also varied by researcher. Previous research has focused mainly on the negative effects of transmitter mass alone on animal welfare and behavior, excluding mass of epoxy applied (Watson & Granger, 1998; Mansfield *et al.*, 2012; Thums *et al.*, 2013). In a worst-case scenario calculated from the mass of epoxy applied to surrogate transmitters, the mass of

a transmitter and largest amount of epoxy on the smallest individual tagged by SCDNR comprises only 2.4% of the total body mass, half of the 5% maximum recommended (Wilson *et al.*, 2002). Therefore, the combined mass of satellite transmitters and epoxy likely has a minimal impact on animal behavior (Wilson *et al.*, 2002; Thums *et al.*, 2013).

While epoxy footprint has been briefly mentioned in previous tagging studies (Seney, 2008; McClellan & Read, 2009; Fujisaki *et al.*, 2016), the present study is the first to empirically test for effects of epoxy footprint on transmitter retention. Epoxy footprint may not influence break force in a laboratory setting for two-component marine epoxy adhered to ceramic tile. Both footprints withstood the maximum load for the entire trial duration, with no detachments for either transmitter size. Contrary to published studies for other epoxies and substrata (Zhai *et al.*, 2006; Anagreh & Robaidi, 2010), larger surface areas were not associated with increased adhesion of two-component epoxies in the present study. Despite the lack of detachments, future studies should not consider using greater force to induce detachment with the force apparatus used in the present study given that eye-screws began to deform with additional weights.

Surface impurities on tile substrata as well as improper epoxy curing may have influenced epoxy adhesion. Although studies on the effect of surface impurities on epoxy adhesion to hard-shelled sea turtle keratin have not been conducted, studies in materials science indicate that shear stress is a function of the presence of surface impurities (Williams, 1964; Stein, 1967; Tang *et al.*, 2012). Generally, shear strength decreases with increasing presence of surface impurities (Stein, 1967). In the present study, attempts were made to remove surface impurities on tiles, but sanding was not deemed necessary to smooth surfaces. However, impurities remaining on tile surfaces possibly affected

epoxy adhesion. Thus, conclusions regarding surrogate transmitter adhesion to tile may be limited. Adhesion may have also been influenced by improper curing of the epoxy itself. Seney *et al.* (2010) recommends discarding initial "squeezes" from the epoxy mixing nozzle to ensure proper curing when utilizing Power-Fast two-part epoxy (*i.e.*, the epoxy used in the current study). Since such practices were not employed in the current study, epoxy may not have cured properly, possibly influencing epoxy adhesion. However, given epoxy application procedures were consistent across replicates and a majority of detachments occurred on frame 4, tile preparation and epoxy application appear to be less likely culprits in surrogate transmitter detachment.

A possible limitation of the current study is that variability in epoxy thickness influenced adhesion strength. Despite efforts to limit variation in epoxy thickness, studies in material science generally show that variability in adhesive thickness on a millimeter scale can significantly affect shear strength (Arici *et al.*, 2005; da Silva *et al.*, 2006; Yeon *et al.*, 2019). The relationship between adhesive thickness and shear stress depends on type of adhesive used (da Silva *et al.*, 2006). For example, theory dictates that brittle adhesives with no plasticity should display positive associations between adhesive thickness and bond strength, while ductile adhesives (*i.e.*, Hysol EA 9361 from Loctite, Munich, Germany) should display inverse associations (Crocombe, 1989; da Silva *et al.*, 2006). Given the brittle nature of cured two-component epoxy used in the current study, thicker layers of applied epoxy may yield higher shear strengths. However, empirical testing is needed to examine the influence of thickness of two-component marine epoxy on transmitter adhesion. Future studies may benefit from using a metric encompassing

the combined height of a surrogate transmitter and thickness of epoxy applied to examine the effects on shear strength in a laboratory setting.

The current study provides the first documentation of the effects of submergence in seawater on surrogate transmitter retention. *In situ* transmitter retention was unrelated to epoxy footprint and mass of epoxy applied. No difference was detected in the number of attached surrogate transmitters by epoxy footprint across monitor dates. However, future studies should consider including additional replicates given the relatively few numbers of detachments observed. Epoxy mass varied significantly among researchers for both transmitter sizes; however, small transmitter detachment did not reflect epoxy mass. This suggests variation in the amount of epoxy applied among researchers may not influence transmitter retention, but further testing with additional replicates is needed. It should be noted that the amount of epoxy applied should be minimized since the build-up of epoxy under transmitters can increase drag (Jones *et al.*, 2013).

A majority of surrogate transmitters detachments occurred following 29 days of submersion in seawater, possibly indicating that transmitter attachments tend to fail early rather than late in field conditions. A previous study reported epoxy resins used in construction applications decreased in shear strength following 16 days of submersion in seawater (Doyle & Pethrick, 2009). Decreases in shear strength are likely explained by seawater plasticizing the epoxy resin, allowing for continued ingress of seawater and subsequent bond degradation (Doyle & Pethrick, 2009). A similar mechanism of epoxy degradation in seawater observed by Doyle and Pethrick (2009) may partially explain reduced adhesion and detachment of surrogate transmitters. Further study is needed on the effects and mechanisms of seawater submersion on adhesion strength of two-

component marine epoxy. Given *in situ* transmitter retention was unrelated to epoxy footprint and mass of epoxy applied, additional reasons for premature detachment in the current study may include insufficient attachment.

The effect of carapace morphology, namely carapace angle, on transmitter adhesion to hard-shelled sea turtles remains poorly understood. Given transmitters do not always fully adhere against the curved carapaces of hard-shelled sea turtles (Mansfield *et al.*, 2012), gaps between the carapace and adhesives may result in transmitter detachment (Seney, 2008). As such, carapace curvature may conceivably contribute to reduced transmitter adhesion. However, no epoxy detachments occurred for either simulated carapace angle in the present study. One possible explanation may be that simulated carapace angle calculated in this study was an oversimplified representation of carapace curvature. Future studies using alternative metrics of carapace curvature may be useful to better understand the effects of carapace morphology among other species-specific factors on transmitter adhesion to hard-shelled sea turtles. In addition to premature detachment, other factors that influence transmission loss include fouling on transmitters.

Biofouling was significantly different between surfaces of interest but not monitor dates for tile replicates, indicating that biofouling occurs at different rates for various substrate types. As predicted, percent cover was significantly lower on wooden block compared with tile and epoxy for both monitor dates, likely due to the application of anti-fouling paint. Wooden block was the only surface to significantly increase in percent cover between monitor dates given that all other surfaces were essentially saturated with epibiota by the first monitor date. Another possible explanation is the anti-fouling paint began to wear off, decreasing effectiveness at preventing biofouling accumulation over

time. Copper-based anti-fouling paints, such as the one used in the current study, are reportedly highly variable in their effectiveness (Bleile & Rodgers, 2001).

Since observed biofouling was low on surrogate transmitters, biofouling-induced saltwater switch hijacking may be a less likely source of transmission loss for shorter track durations. Transmission loss can occur when biofouling accumulation on the saltwater switches of transmitters falsely indicates submergence (Seney, 2008). In the present study, mean percent cover of biofouling epibiota on surrogate transmitters (*i.e.*, wooden blocks) was low following approximately two months of submergence. Low biofouling may be explained by temporal implications of biofouling given the intensity of fouling varies with season (Wahl & Lafargue, 1990; Abdelsalam & Abdel Wahab, 2012). This finding is corroborated by a previous study conducted during a temporal frame comparable to the present study (August to November; Seney, 2008). Seney (2008) demonstrated that little to no epibiota colonized surrogate transmitters coated with anti-fouling paint following submersion for approximately three months. This suggests saltwater switch hijacking induced by biofouling accumulation is an unlikely culprit for transmission failure for track durations of approximately two months or less.

Surrogate transmitters affixed to the seafloor were generally representative of transmitters attached to loggerhead sea turtles with respect to depth and seasonal mobility. Surrogate transmitter submersion depth (17 m) falls well within the range of depths adult male (Arendt, Segars, Byrd, Boynton, Schwenter, *et al.*, 2012) and juvenile (Arendt, Segars, Byrd, Boynton, Whitaker, *et al.*, 2012) loggerheads have previously been tracked during the summer off the southeastern U.S. The submersion depth in this study is also comparable to the depth at which juvenile and adult male loggerheads have

been captured in trawl surveys (Arendt, Boynton, *et al.*, 2012). Previous studies have reported a highly localized nature of juvenile (Arendt, Segars, Byrd, Boynton, Whitaker, *et al.*, 2012) and adult male (Arendt, Segars, Byrd, Boynton, Schwenter, *et al.*, 2012) loggerheads during the summer/fall foraging season.

An additional limitation of the experimental design includes the effect of substrate movement on the accumulation and composition of biofouling communities on surrogate transmitters. Biofouling assemblages develop differently depending on substrate movement (Wahl & Lafargue, 1990; Glasby, 2001). A previous study demonstrated that the movement of a hard substrate influenced biofouling composition over a period of seven months, with two- to three-fold more biomass accumulation on moving substrata compared with stationary (Glasby, 2001). One explanation may be that transmitters adhered to mobile sea turtles potentially encounter a greater diversity of water masses and associated larva compared with surrogate transmitters in a fixed location; however, studies on the effects of Eulerian vs. Lagrangian movement on associated epibiota are not readily available. Differences in water flow between fixed and moving surfaces may also explain this phenomenon given that water flow influences the settlement and development of many marine invertebrates (Mullineaux & Garland, 1993; Eckman & Duggins, 1993; Glasby, 2001). Thus, differences in flow between fixed and moving surfaces may cause differences in the accumulation and composition of biofouling communities (Glasby, 2001). Therefore, biofouling on stationary surrogate transmitters may not be fully representative of fouling on transmitters attached to loggerheads.

Satellite transmitters adhered to sea turtles experience a number of forces that stationary surrogate transmitters may not—including drag, unnatural impact (*i.e.*,

interaction with watercraft or TEDs), and natural impact (*i.e.*, wedging/grooming behavior, mating). Sea turtles fitted with transmitters experience increased drag forces due to the rectangular shape of most backpack-style transmitters, which increases the animal's frontal area (Watson & Granger, 1998; Jones *et al.*, 2013). A previous empirical study reported most transmitters cause approximately 5% additional drag to adult sea turtles, while the same devices on juveniles increase drag by over 100% (Jones *et al.*, 2013). Unnatural impacts, such as interactions with TEDs or watercraft, are another source of force that may contribute to weakened epoxy adhesion. Although studies on the effect of watercraft interactions on transmitter adhesion are limited, Seney (2008) notes that transmitter detachment possibly results from events such as boat strikes or movement through a TED. In experiments with captive-reared juvenile loggerheads, transmitters on several individuals temporarily wedged between TED bars during escape (Seney, 2008). Despite that no detachments occurred (Seney, 2008), wedging of transmitters in TEDs conceivably contributes to reduced epoxy adhesion to hard-shelled sea turtles.

Natural impacts, such as wedging and grooming behaviors as well as mating behaviors, are also a source of blunt force to transmitters adhered to hard-shelled sea turtles. Loggerheads reportedly wedge and groom against hard substrata (Caine, 1986; Watson & Granger, 1998; Seney, 2008), thereby damaging transmitters (Hays *et al.*, 2007) and potentially weakening the epoxy bond to the carapace. For example, a captive-reared loggerhead was previously observed rubbing against a piling; within four hours, the surrogate transmitter was found detached at the piling's base (Seney, 2008). Mating interactions are reported as a primary source of tag loss for female leatherbacks given the contact between the plastrons of males and the carapaces of females during copulation

(Hamelin & James, 2018). Such behaviors may induce tag loss for female loggerheads as well given the similar mounting behaviors during courtship (Frick *et al.*, 2000; Merino-Zavala *et al.*, 2018) and the generally aggressive nature of copulation (Schofield *et al.*, 2006). Male loggerheads may also experience transmitter detachment during mating interactions due to physical interference from attendant males (Schofield *et al.*, 2006).

Continued research is warranted to identify alternative epoxies that provide superior adhesion with the smallest possible epoxy footprint to reduce drag. Identification of such epoxies may allow transmitters to adhere to hard-shelled sea turtles for longer periods of time, potentially increasing track durations and data collection. The build-up of adhesives along with transmitter shape can increase the transmitter profile and in turn the animal's frontal area (Jones *et al.*, 2013), thus increasing drag (Watson & Granger, 1998). Although typically used to track immature individuals, transmitter miniaturization may help relieve hydrodynamic problems for larger individuals in the future. For example, small solar-powered tags (38 mm length × 17 mm width × 12 mm height) that have been used to track neonate loggerheads (Mansfield *et al.*, 2012) require conceivably less amounts of adhesive compared with standard-sized transmitters. Therefore, epoxies that can be applied with a minimal epoxy footprint and thickness may help alleviate drag forces (Jones *et al.*, 2013). Continued improvements in satellite transmitter technology and attachment methods may extend track durations while simultaneously minimizing negative impacts on animal welfare (Watson & Granger, 1998; Hays *et al.*, 2007).

FIGURES

Figure 4.1. Experimental units with small (left) and large (right) surrogate transmitters affixed to tile 1. Small wooden blocks correspond to SPOT and TAM-4310 transmitters; large blocks correspond to ST-20 and TAM-4525 transmitters. Epoxy extends in four cm arc beyond edge of block, denoted by red lines.

Figure 4.2. Side view of the force apparatus employed in full-scale testing with several 4.5 kg weights loaded onto bottom weight tray. Replicates were secured onto the force apparatus by a pivoting wooden block to a wooden surface with adjustable inclines. The weight tray was attached by rope and S-hook to eye-screws mounted in each experimental unit. Rope passed through a safety visor, which served to protect researchers during trials.

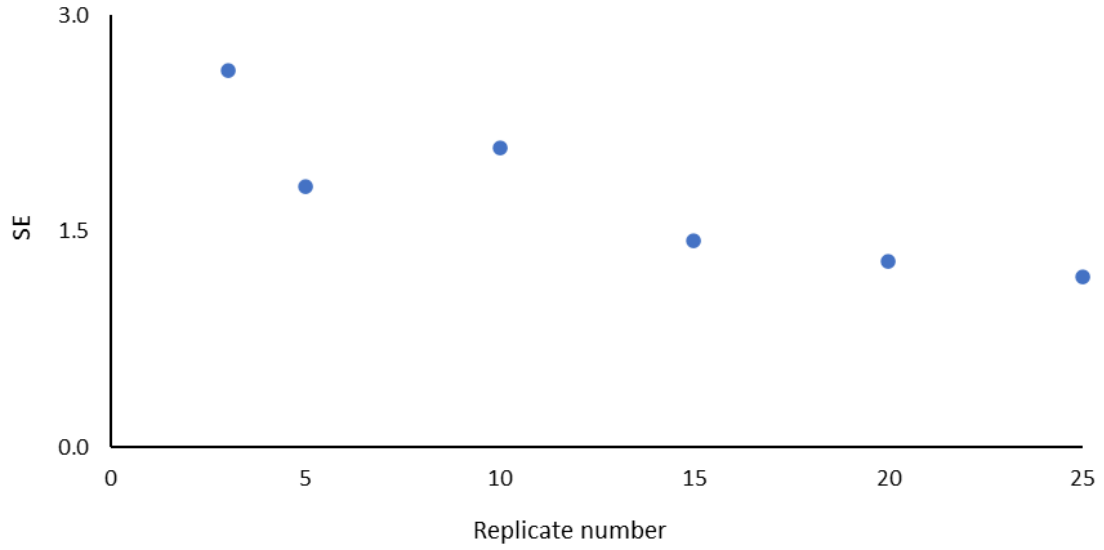

Figure 4.3. Standard error (y-axis) of the break force (N) of laminate flooring for various numbers of replicates (x-axis).

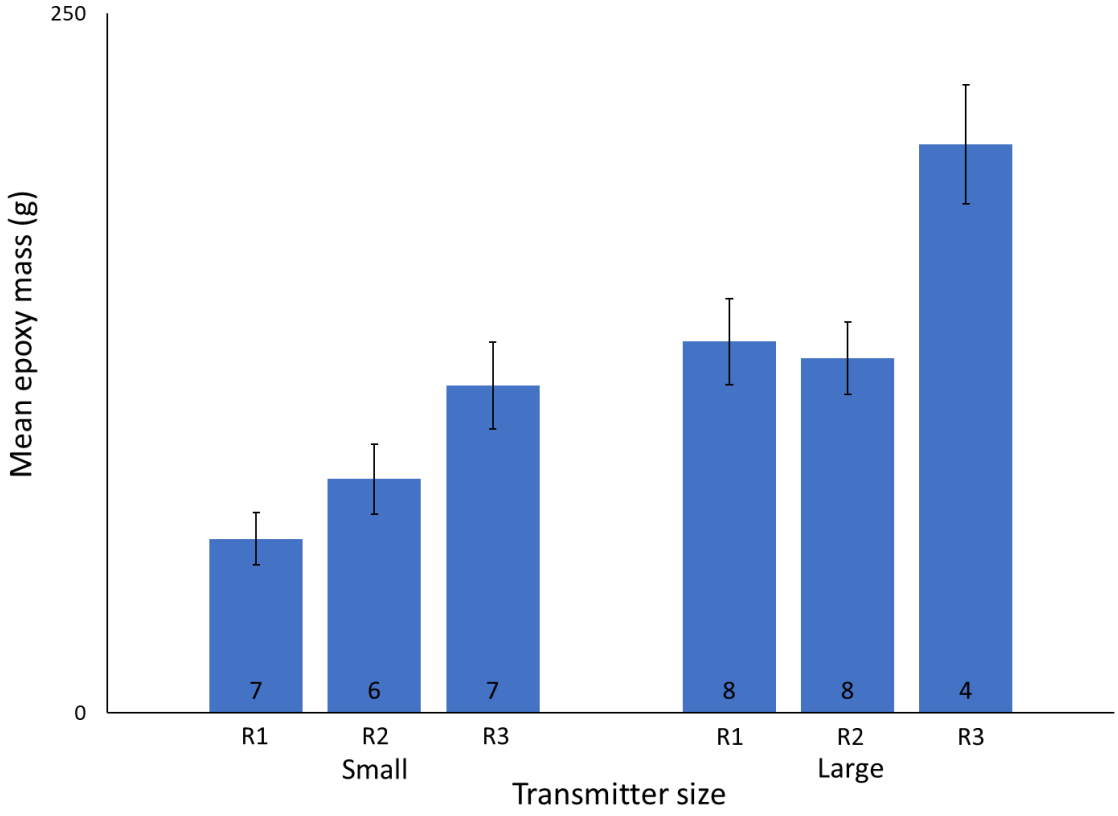

Figure 4.4. Mean epoxy masses (y-axis) by researcher (R1, R2, R3) and transmitter size (x-axis). Error bars correspond to 95% confidence intervals. Numbers at base of bars correspond to sample size.

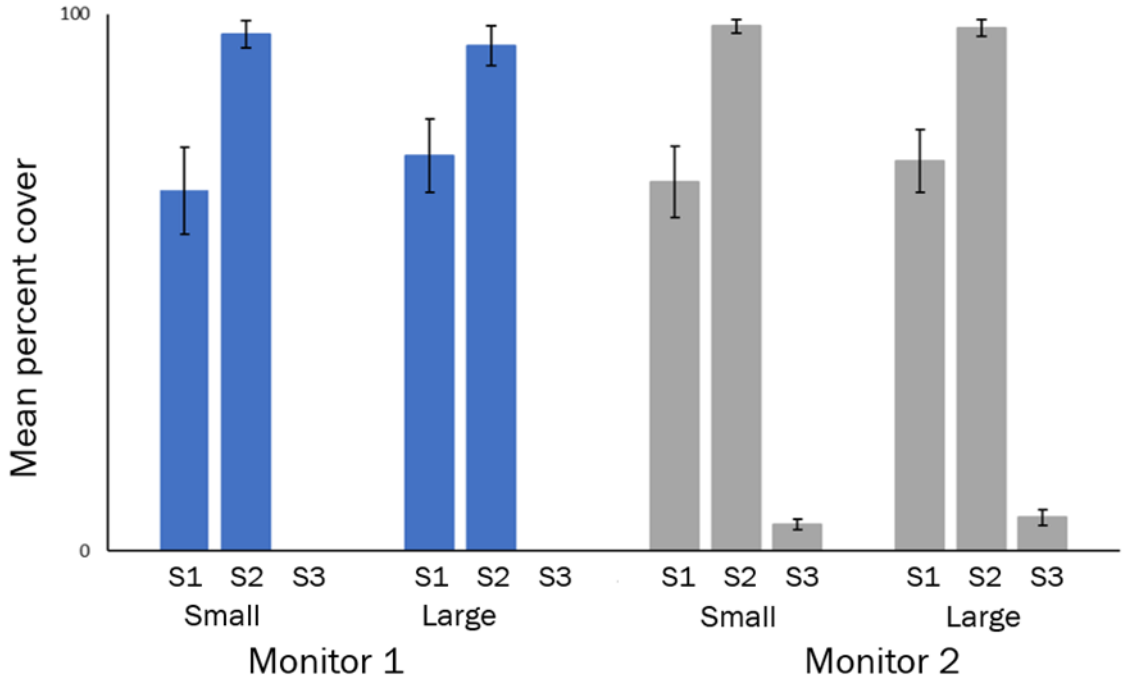

Figure 4.5. Mean percent biofouling cover (y-axis) by monitor date (x-axis) and surrogate transmitter size on surfaces of interest (S1, S2, S3) for tile replicates. Error bars are standard error. S1 corresponds to tile, S2 to epoxy, and S3 to wooden block.

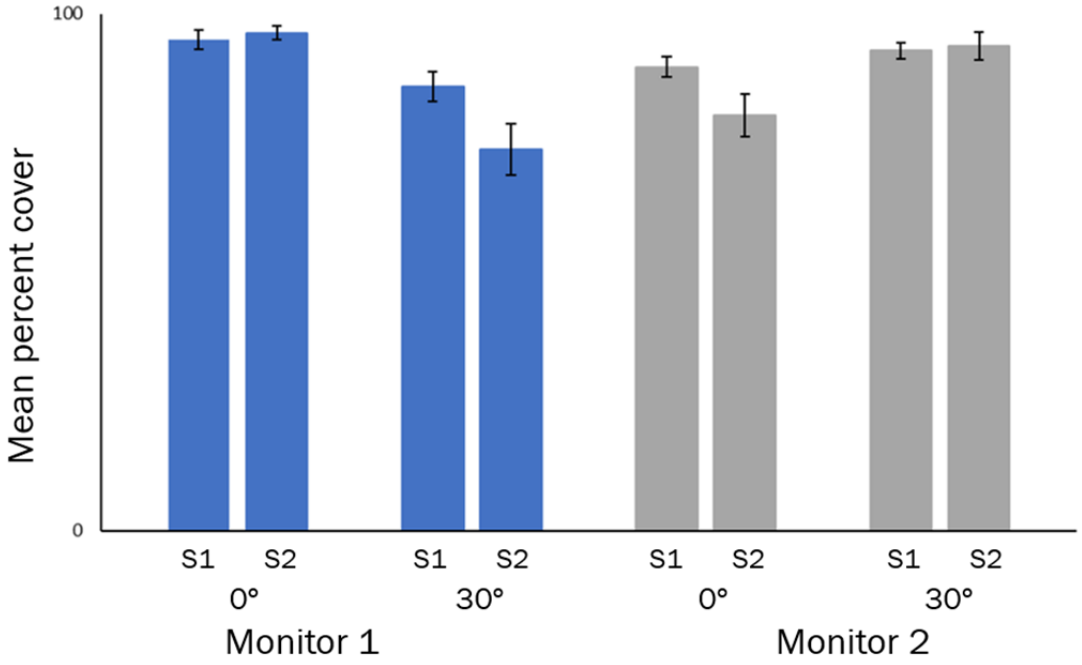

Figure 4.6. Mean percent biofouling cover (y-axis) by monitor date (x-axis) and simulated carapace angles on surfaces of interest (S1, S2) for laminate flooring replicates. Error bars are standard error. S1 corresponds to laminate flooring, and S2 to epoxy.

CHAPTER 5. GENERAL CONCLUSIONS

The present multidisciplinary study was initiated to identify factors influencing track duration disparities observed for loggerhead sea turtles. Transmitter adhesion to loggerhead keratin and subsequent track durations are likely influenced by a combination of the physical and biochemical properties of keratin as well as the mechanical properties of epoxy. Physical properties of loggerhead keratin and mechanical properties of epoxy suggest transmitter detachment may be implicated for shorter track durations. Despite consistency in epoxy application across scute subsamples, epoxy adhesion strength to loggerhead keratin was highly variable between and within individuals. Variability in epoxy adhesion may be explained in part by variability observed in scute thickness. As such, no reliable predictor for epoxy detachment was identified. A majority of surrogate transmitters detached following 29 days of submersion in seawater, suggesting epoxy attachments tend to fail early rather than late *in situ*. Therefore, epoxy and transmitter detachment cannot be ruled out as a source of transmission failure for satellite track durations of one month or less for loggerhead sea turtles.

Biochemical properties of keratin cannot be ruled out as a contributing factor in transmitter detachment given specific fatty acids may influence epoxy adhesion strength. Arachidic acid may play an important role in forming a water-loss barrier that possibly influences transmitter adhesion. While the role of arachidic acid in loggerhead keratin

remains largely unknown, it may perform a similar water-loss barrier function to that of MEA in mammalian keratin (*i.e.*, hair fibers; Jones & Rivett, 1997). This water-loss barrier may influence the ability of epoxy to bond to the carapace, but additional research is needed. In addition, increasing percentages of palmitoleic acid were associated with decreasing mean break forces across individuals. Further study is needed to validate the location of fatty acids within loggerhead keratin layers to fully understand the influence of scute biochemical composition on transmitter adhesion.

Saltwater switch hijacking due to biofouling is a less likely source of transmission loss for shorter track durations for transmitters deployed during fall. Observed percent cover of biofouling epibiota was low on surrogate transmitters, which may be explained by generally greater biofouling accumulation reported in spring and summer months (Mazouni *et al.*, 2001; Abdelsalam & Abdel Wahab, 2012). The application of anti-fouling paint may also have reduced biofouling accumulation observed on surrogate transmitters. Seney (2008) also reported little to no biofouling accumulation on surrogate transmitters coated with anti-fouling paint following submersion for approximately three months during fall. Although precise reasons for transmission failure may not be possible to decipher in every case, identifying causes of transmission loss serves to direct future improvements in satellite transmitter attachment techniques (Hays *et al.*, 2007).

While the current study provides the first documentation of epoxy adhesion strength on and fatty acids present in the carapacial scutes of loggerhead sea turtles, further research is needed on the physical and biochemical properties of hard-shelled sea turtle keratin. Additional study is warranted to capture a broader range of epoxy adhesion strength to loggerhead keratin since adhesion strength was underestimated for scutes

where no detachment occurred. Given only loggerheads were available for sampling in this study, sampling additional hard-shelled sea turtle species may be useful to quantify and compare epoxy adhesion across species. The effects of carapace morphology on epoxy adhesion remain unclear and thus warrant continued investigation using alternative metrics of carapace curvature. Additional research is also needed to assess the role of arachidic acid in forming a water-loss barrier in loggerhead keratin and its influence on epoxy adhesion. Validating the location of fatty acids within loggerhead keratin may help researchers better understand the role of fatty acids in transmitter adhesion.

Continued study is also needed on the mechanical properties of epoxy separate from scute biochemical composition. Future simulation experiments using more realistic sea turtle keratin substitute materials following keratin preparation protocol may provide more conclusive results on transmitter adhesion. Including additional replicates in submersion experiments may reduce sample size effects observed in the present study to better understand the role of epoxy footprint on transmitters adhesion. Research investigating potential mechanisms of epoxy degradation in seawater may serve to provide estimates of epoxy attachment duration *in situ*. Finally, further study is warranted to identify alternative epoxies that provide superior adhesion with a minimal epoxy footprint to reduce drag. Understanding the physical, biochemical, and mechanical properties of both loggerhead keratin and epoxies used to attach satellite transmitters may ultimately lead to future improvements in transmitter adhesion for loggerhead sea turtles.

LITERATURE CITED

Abdelsalam, K. M., & Abdel Wahab, M. M. (2012). Effects of Depth and Orientation on Marine Fouling Assemblages in the Coastal Waters of Abu Qir Harbor, Egypt. *Journal of King Abdulaziz University*, *23*(2), 3–24. https://doi.org/10.4197/Mar

Ackman, R. G., Hooper, S. N., & Sipos, J. C. (1972). Distribution of trans-6-hexadecenoic and other fatty acids in tissues and organs of the atlantic leatherback turtle Dermochelys coriacea coriacea L. *International Journal of Biochemistry*. https://doi.org/10.1016/0020-711X(72)90076-6

Alibardi, L., & Thompson, M. B. (1999). Epidermal differentiation during carapace and plastron formation in the embryonic turtle Emydura macquarii. *Journal of Anatomy*, *194*(4), 531–545. https://doi.org/10.1017/S002187829900494X

Alibardi, L., & Toni, M. (2006a). Cytochemical, biochemical and molecular aspects of the process of keratinization in the epidermis of reptilian scales. *Progress in Histochemistry and Cytochemistry*, *40*(2), 73–134. https://doi.org/10.1016/j.heares.2006.01.005

Alibardi, L., & Toni, M. (2006b). Immunolocalization and characterization of beta-keratins in growing epidermis of chelonians. *Tissue and Cell*, *38*(1), 53–63. https://doi.org/10.1016/j.tice.2005.11.001

Alibardi, L., & Toni, M. (2006c). Skin structure and cornification proteins in the soft-shelled turtle Trionyx spiniferus. *Zoology*, *109*(3), 182–195. https://doi.org/10.1016/J.ZOOL.2005.11.005

Anagreh, N., & Robaidi, A. Al. (2010). Improvement in Adhesion Behavior of Aluminum Due to Surfaces Treatment with Arc Discharge. *Jordan Journal of Mechanical and Industrial Engineering*, *4*(2), 330–339.

AOAC. (2002). AOAC Official method 996.06: Fat (total, saturated, and unsaturated) in foods - Hydrolytic Extraction Gas Chromatographic method. *AOAC International*.

Appelquist, H., Asbirk, S., & Drabæk, I. (1984). Mercury monitoring: Mercury stability in bird feathers. *Marine Pollution Bulletin*, *15*(1), 22–24. https://doi.org/10.1016/0025-326X(84)90419-3

Arendt, M. D., Boynton, J., Schwenter, J., Byrd, J., Segars, A., Whitaker, J., Parker, L., Owens, D., Blanvillain, G., Quattro, J., & Roberts, M. (2012). Spatial clustering of loggerhead sea turtles in coastal waters of the NW Atlantic Ocean: implications for management surveys. *Endangered Species Research*, *18*(3), 219–231. https://doi.org/10.3354/esr00450

Arendt, M. D., Segars, A. L., Byrd, J. I., Boynton, J., Schwenter, J. A., Whitaker, J. D., & Parker, L. (2012). Migration, distribution, and diving behavior of adult male loggerhead sea turtles (Caretta caretta) following dispersal from a major breeding aggregation in the Western North Atlantic. *Marine Biology*, *159*(1), 113–125. https://doi.org/10.1007/s00227-011-1826-0

Arendt, M. D., Segars, A. L., Byrd, J. I., Boynton, J., Whitaker, J. D., Parker, L., Owens,

D. W., Blanvillain, G., Quattro, J. M., & Roberts, M. A. (2012). Seasonal distribution patterns of juvenile loggerhead sea turtles (Caretta caretta) following capture from a shipping channel in the Northwest Atlantic Ocean. *Marine Biology*, *159*(1), 127–139. https://doi.org/10.1007/s00227-011-1829-x

Arici, S., Caniklioglu, C. M., Arici, N., Ozer, M., & Oguz, B. (2005). Adhesive thickness effects on the bond strength of a light-cured resin-modified glass ionomer cement. *Angle Orthodontist*, *75*(2), 254–259. https://doi.org/10.1043/0003-3219(2005)075<0250:ATEOTB>2.0.CO;2

Asi, I. M. (2007). Evaluating skid resistance of different asphalt concrete mixes. *Building and Environment*, *42*(1), 325–329. https://doi.org/10.1016/j.buildenv.2005.08.020

Bailey, N. T. J. (1951). On Estimating the Size of Mobile Populations from Recapture Data Published by : Oxford University Press on behalf of Biometrika Trust Stable URL : http://www.jstor.org/stable/2332575 Accessed : 14-06-2016 05 : 38 UTC. *Biometrika*, *38*(3), 293–306.

Bakar, K., Mohamad, H., Latip, J., Tan, H. S., & Herng, G. M. (2017). Fatty acids compositions of Sargassum granuliferum and Dictyota dichotoma and their anti-fouling activities. *Journal of Sustainability Science and Management*, *12*(2), 8–16.

Blau, P. J. (2001). The significance and use of the friction coefficient. *Tribology International*, *34*(9), 585–591. https://doi.org/10.1016/S0301-679X(01)00050-0

Bleile, H., & Rodgers, S. D. (2001). Marine Coatings. In *Encyclopedia of Materials: Science and Technology* (Second, pp. 5174–5185). Elsevier. https://doi.org/10.1016/b0-08-043152-6/00899-8

Bligh, E. G., & Dyer, W. J. (1959). Canadian Journal of Biochemistry and Physiology. *Canadian Journal of Biochemistry and Physiology*, *37*(8), 911–917.

Bozcali, E., Süzer, O., Gürsoy, H. N., Atukeren, P., & Gümüstas, K. M. (2009). Effects of erucic acid supplemented feeding on chronic doxorubucin toxicity in rats. *International Journal of Clinical and Experimental Medicine*, *2*(4), 337–347. http://www.ncbi.nlm.nih.gov/pubmed/20057977

Caine, E. A. (1986). Carapce Epibionts of Nesting Loggerhead Sea Turtles: Atlantic Coast of U.S.A. In *Journal of Experimental Marine Biology and Ecology* (Vol. 95, pp. 15–26).

Casale, P., Freggi, D., Rigoli, A., Ciccocioppo, A., & Luschi, P. (2017). Geometric morphometrics, scute patterns and biometrics of loggerhead turtles (Caretta caretta) in the central Mediterranean. *Amphibia Reptilia*, *38*(2), 145–156. https://doi.org/10.1163/15685381-00003096

Chaloupka, M., Parker, D., & Balazs, G. (2004). Modelling post-release mortality of loggerhead sea turtles exposed to the Hawaii-based pelagic longline fishery. *Marine Ecology Progress Series*, *280*, 285–293. https://doi.org/10.3354/meps280285

Chong, J., Soufan, O., Li, C., Caraus, I., Li, S., Bourque, G., Wishart, D. S., & Xia, J. (2018). MetaboAnalyst 4.0: Towards more transparent and integrative metabolomics

analysis. *Nucleic Acids Research*, *46*(W1), W486–W494. https://doi.org/10.1093/nar/gky310

Coleman, A. T., Pitchford, J. L., Bailey, H., & Solangi, M. (2017). Seasonal movements of immature Kemp's ridley sea turtles (Lepidochelys kempii) in the northern gulf of Mexico. *Aquatic Conservation: Marine and Freshwater Ecosystems*, *27*(1), 253–267. https://doi.org/10.1002/aqc.2656

Crocombe, A. D. (1989). Global yielding as a failure criterion for bonded joints. *International Journal of Adhesion and Adhesives*, *9*(3), 145–153. https://doi.org/10.1016/0143-7496(89)90110-3

Da Silva, A. C. C. D., Dos Santos, E. A. P., Das, F. L., Weber, M. I., Batista, J. A. F., Serafini, T. Z., & De Castilhos, J. C. (2011). Satellite-tracking reveals multiple foraging strategies and threats for olive ridley turtles in Brazil. *Marine Ecology Progress Series*, *443*(Bolten 2003), 237–247. https://doi.org/10.3354/meps09427

da Silva, L. F. M., Rodrigues, T. N. S. S., Figueiredo, M. A. V., de Moura, M. F. S. F., & Chousal, J. A. G. (2006). Effect of adhesive type and thickness on the lap shear strength. *Journal of Adhesion*, *82*(11), 1091–1115. https://doi.org/10.1080/00218460600948511

Dalla Valle, L., Nardi, A., Toni, M., Emera, D., & Alibardi, L. (2009). Beta-keratins of turtle shell are glycine-proline-tyrosine rich proteins similar to those of crocodilians and birds. *Journal of Anatomy*, *214*(2), 284–300. https://doi.org/10.1111/j.1469-7580.2008.01030.x

Davidson, B. C., Ayvazyan, A., Evani, S., & Cliff, G. (2014). Comparison of the fatty acid profiles of liver and fat from five Indian Ocean loggerhead turtles (C *aretta caretta*). *Journal of the Marine Biological Association of the United Kingdom*, *94*(7), 1581–1584. https://doi.org/10.1017/S0025315414000484

Day, R. D., Christopher, S. J., Becker, P. R., & Whitaker, D. W. (2005). Monitoring mercury in the loggerhead sea turtle, Caretta caretta. *Environmental Science and Technology*, *39*(2), 437–446. https://doi.org/10.1021/es049628q

Doyle, G., & Pethrick, R. A. (2009). Environmental effects on the ageing of epoxy adhesive joints. *International Journal of Adhesion and Adhesives*, *29*(1), 77–90. https://doi.org/10.1016/j.ijadhadh.2008.02.001

Eckert, S. A., & Eckert, K. L. (1986). *MTN 37:1-3 Harnessing Leatherbacks*. Marine Turtles Newsletter 37:1-3. http://www.seaturtle.org/mtn/archives/mtn37/mtn37p1.shtml?nocount

Eckman, J. E., & Duggins, D. O. (1993). Effects of Flow Speed on Growth of Benthic Suspension Feeders. *The Biological Bulletin*, *185*(1), 28–41. https://doi.org/10.2307/1542128

Espinoza, E. O., Baker, B. W., & Berry, C. A. (2007). The analysis of sea turtle and bovid keratin artefacts using drift spectroscopy and discriminant analysis. *Archaeometry*, *49*(4), 685–698. https://doi.org/10.1111/j.1475-4754.2007.00328.x

Frick, M. G., Slay, C. K., Quinn, C. A., Windham-reid, A., Duley, P. A., Ryder, C. M., & Morse, L. J. (2000). Aerial Observations of Courtship Behavior in Loggerhead Sea Turtles (Caretta caretta) from Southeastern Georgia and Northeastern Florida. *Journal of Herpetology*, *34*(1), 153–158.

Fujisaki, I., Hart, K., & Sartain-Iverson, A. (2016). Habitat selection by green turtles in a spatially heterogeneous benthic landscape in Dry Tortugas National Park, Florida. *Aquatic Biology*, *24*(3), 185–199. https://doi.org/10.3354/ab00647

Fuller, W. J., Broderick, A. C., Enever, R., Thorne, P., & Godley, B. J. (2010). Motile homes: A comparison of the spatial distribution of epibiont communities on Mediterranean sea turtles. *Journal of Natural History*, *44*(27), 1743–1753. https://doi.org/10.1080/00222931003624820

Glasby, T. M. (2001). Development of sessile marine assemblages on fixed versus moving substrata. *Marine Ecology Progress Series*, *215*, 37–47. https://doi.org/10.3354/meps215037

Godley, B., Lima, E., Åkesson, S., Broderick, A., Glen, F., Godfrey, M., Luschi, P., & Hays, G. (2003). Movement patterns of green turtles in Brazilian coastal waters described by satellite tracking and flipper tagging. *Marine Ecology Progress Series*, *253*, 279–288. https://doi.org/10.3354/meps253279

Gonçalves-de-Albuquerque, C. F., Silva, A. R., Burth, P., Castro-Faria, M. V., & Castro-Faria-Neto, H. C. (2016). Oleic Acid and Lung Injury. In *Handbook of Lipids in Human Function* (pp. 605–634). AOCS Press. https://doi.org/10.1016/B978-1-63067-036-8.00023-8

Griffin, D. B. B., Murphy, S. R., Frick, M. G., Broderick, A. C., Coker, J. W., Coyne, M. S., Dodd, M. G., Godfrey, M. H., Godley, B. J., Hawkes, L. A., Murphy, T. M., Williams, K. L., & Witt, M. J. (2013). Foraging habitats and migration corridors utilized by a recovering subpopulation of adult female loggerhead sea turtles: Implications for conservation. *Marine Biology*, *160*(12), 3071–3086. https://doi.org/10.1007/s00227-013-2296-3

Grönqvist, R., Hirvonen, M., Rajamäki, E., & Matz, S. (2003). The validity and reliability of a portable slip meter for determining floor slipperiness during simulated heel strike. *Accident Analysis & Prevention*, *35*(2), 211–225. https://doi.org/10.1016/S0001-4575(01)00105-1

Guitart, R., Silvestre, A. M., Guerrero, X., & Mateo, R. (1999). Comparative study on the fatty acid composition of two marine vertebrates: striped dolphins and loggerhead turtles. *Comparative Biochemistry and Physiology Part B: Biochemistry and Molecular Biology*, *124*(4), 439–443. https://doi.org/10.1016/S0305-0491(99)00138-8

Hamelin, K. M., & James, M. C. (2018). Evaluating outcomes of long-term satellite tag attachment on leatherback sea turtles. *Animal Biotelemetry*, *6*(1), 1–14. https://doi.org/10.1186/s40317-018-0161-3

Hart, K. M., & Hyrenbach, K. D. (2010). Satellite telemetry of marine megavertebrates:

The coming of age of an experimental science. *Endangered Species Research*, *10*(1), 9–20. https://doi.org/10.3354/esr00238

Hawkes, L. A., Tomás, J., Revuelta, O., León, Y., Blumenthal, J., Broderick, A., Fish, M., Raga, J., Witt, M., & Godley, B. (2012). Migratory patterns in hawksbill turtles described by satellite tracking. *Marine Ecology Progress Series*, *461*, 223–232. https://doi.org/10.3354/meps09778

Hays, G., Bradshaw, C. J. A., James, M. C., Lovell, P., & Sims, D. W. (2007). Why do Argos satellite tags deployed on marine animals stop transmitting? *Journal of Experimental Marine Biology and Ecology*, *349*(1), 52–60. https://doi.org/10.1016/J.JEMBE.2007.04.016

Hays, G., Broderick, A., Godley, B., Luschi, P., & Nichols, W. (2003). Satellite telemetry suggests high levels of fishing-induced mortality in marine turtles. *Marine Ecology Progress Series*, *262*, 305–309. https://doi.org/10.3354/meps262305

Hays, G., Hobson, V. J., Metcalfe, J. D., Righton, D., & Sims, D. W. (2006). Flexible foraging movements of leatherback turtles across the North Atlantic ocean. *Ecology*, *87*(10), 2647–2656. https://doi.org/10.1890/0012-9658(2006)87[2647:FFMOLT]2.0.CO;2

Hays, G., Houghton, J. D. R., Isaacs, C., King, R. S., Lloyd, C., & Lovell, P. (2004). First records of oceanic dive profiles for leatherback turtles, Dermochelys coriacea, indicate behavioural plasticity associated with long-distance migration. *Animal Behaviour*, *67*(4), 733–743. https://doi.org/10.1016/j.anbehav.2003.08.011

Hernandez, E. M. (2016). Specialty Oils: Functional and Nutraceutical Properties. In *Functional Dietary Lipids* (pp. 69–101). Woodhead Publishing. https://doi.org/10.1016/B978-1-78242-247-1.00004-1

Houtsmuller, U. M. T., Struijk, C. B., & Van Der Beek, A. (1970). Decrease in rate of ATP synthesis of isolated rat heart mitochondria induced by dietary erucic acid. *Biochimica et Biophysica Acta*, *218*, 564–566.

Jacobi, C. M., & Langevin, R. (1996). Habitat geometry of benthic substrata: Effects on arrival and settlement of mobile epifauna. *Journal of Experimental Marine Biology and Ecology*, *206*(1–2), 39–54. https://doi.org/10.1016/S0022-0981(96)02605-6

Jagdale, G. B., & Gordon, R. (1997). Effect of temperature on the composition of fatty acids in total lipids and phospholipids of entomopathogenic nematodes. *Journal of Thermal Biology*, *22*(4–5), 245–251. https://doi.org/10.1016/S0306-4565(97)00019-3

Jones, L. N., & Rivett, D. E. (1997). The role of 18-methyleicosanoic acid in the structure and formation of mammalian hair fibres. *Micron*, *28*(6), 469–485. https://doi.org/10.1016/S0968-4328(97)00039-5

Jones, Van Houtan, K. S., Bostrom, B. L., Ostafichuk, P., Mikkelsen, J., Tezcan, E., Carey, M., Imlach, B., & Seminoff, J. A. (2013). Calculating the ecological impacts of animal-borne instruments on aquatic organisms. *Methods in Ecology and*

Evolution, *4*(12), 1178–1186. https://doi.org/10.1111/2041-210X.12109

Joniot, S., Salomon, J. P., Dejou, J., & Grégoire, G. (2006). Use of Two Surface Analyzers to Evaluate the Surface Roughness of Four Esthetic Restorative Materials After Polishing. *Operative Dentistry*, *31*(1), 39–46. https://doi.org/10.2341/04-166

Joseph, J. D., Ackman, R. G., & Seaborn, G. T. (1985). Effect of diet on depot fatty acid composition in the green turtle chelonia mydas. *Comparative Biochemistry and Physiology Part B: Comparative Biochemistry*, *80*(1), 15–22. https://doi.org/10.1016/0305-0491(85)90416-X

Jouventin, P., & Weimerskirch, H. (1990). Satellite tracking of Wandering albatrosses. *Nature*, *343*(6260), 746–748. https://doi.org/10.1038/343746a0

Kok, W.-M., Mainal, A., Chuah, C.-H., & Cheng, S.-F. (2018). Content of Erucic Acid in Edible Oils and Mustard by Quantitative ^{13} C NMR. *European Journal of Lipid Science and Technology*, *120*(3), 1700230. https://doi.org/10.1002/ejlt.201700230

Lepage, G., & Roy, C. C. (1986). Direct transesterification of all classes of lipids in a one-step reaction. *Journal of Lipid Research*, *27*, 114–120.

López-Castro, M., Bjorndal, K., & Bolten, A. (2014). Evaluation of scute thickness to infer life history records in the carapace of green and loggerhead turtles. *Endangered Species Research*, *24*(3), 191–196. https://doi.org/10.3354/esr00593

Luckhurst, B. E., & Luckhurst, K. (1978). Analysis of the influence of substrate variables on coral reef fish communities. *Marine Biology*, *49*(4), 317–323. https://doi.org/10.1007/BF00455026

Mansfield, K. L., Saba, V. S., Keinath, J. A., & Musick, J. A. (2009). Satellite tracking reveals a dichotomy in migration strategies among juvenile loggerhead turtles in the Northwest Atlantic. *Marine Biology*, *156*(12), 2555–2570. https://doi.org/10.1007/s00227-009-1279-x

Mansfield, K. L., Wyneken, J., Rittschof, D., Walsh, M., Lim, C. W., & Richards, P. M. (2012). Satellite tag attachment methods for tracking neonate sea turtles. *Marine Ecology Progress Series*, *457*(Bolten 2003), 181–192. https://doi.org/10.3354/meps09485

Marcovaldi, M., Lopez, G., Soares, L., & López-Mendilaharsu, M. (2012). Satellite tracking of hawksbill turtles Eretmochelys imbricata nesting in northern Bahia, Brazil: turtle movements and foraging destinations. *Endangered Species Research*, *17*(2), 123–132. https://doi.org/10.3354/esr00421

Marr, A. G., & Ingraham, J. L. (1962). Effect of Temperature on the Composition of Fatty Acids in Escherichia coli. *Journal of Bacteriology*, *84*(6), 1260–1267. https://doi.org/10.2118/65-04-09

Matsunaga, T., Takeyama, H., Miura, Y., Yamazaki, T., Furuya, hiroyuki, & Sode, K. (1995). Screening of marine cyanobacteria for high palmitoleic acid production. *FEMS Microbiology Letters*, *133*(1–2), 137–141. https://doi.org/10.1016/0378-1097(95)00350-E

Mauvoisin, D., & Mounier, C. (2011). Hormonal and nutritional regulation of SCD1 gene expression. *Biochimie*, *93*(1), 78–86. https://doi.org/10.1016/j.biochi.2010.08.001

Mazouni, N., Gaertner, J. C., & Deslous-Paoli, J. M. (2001). Composition of biofouling communities on suspended oyster cultures: An in situ study of their interactions with the water column. *Marine Ecology Progress Series*, *214*, 93–102. https://doi.org/10.3354/meps214093

McClellan, C., & Read, A. (2009). Confronting the gauntlet: understanding incidental capture of green turtles through fine-scale movement studies. *Endangered Species Research*, *10*, 165–179. https://doi.org/10.3354/esr00199

McConnell, B. J., Chambers, C., Nicholas, K. S., & Fedak, M. A. (1992). Satellite tracking of grey seals (Halichoerus grypus). *Journal of Zoology*, *226*(2), 271–282. https://doi.org/10.1111/j.1469-7998.1992.tb03839.x

McMullen, R. L., & Kelty, S. P. (2007). Molecular dynamic simulations of eicosanoic acid and 18-methyleicosanoic acid langmuir monolayers. *Journal of Physical Chemistry B*, *111*(37), 10849–10852. https://doi.org/10.1021/jp073697k

Merino-Zavala, A. S., Reséndiz, E., Hernández-Gil, Y., & Lara-Uc, M. M. (2018). First report of courtship and mating behavior by loggerhead sea turtle (Caretta caretta) in the Gulf of Ulloa, Baja California Sur, México. *Latin American Journal of Aquatic Research*, *46*(1), 237–239. https://doi.org/10.3856/vol46-issue1-fulltext-25

Mitchell, S. V. (2000). Use of epoxy in telemeter attachment. In *Proceedings of the Eighteenth International Sea Turtle Symposium* (Issue June, pp. 254–255). http://www.nmfs.noaa.gov/pr/pdfs/species/turtlesymposium1998.pdf

Morreale, S. J., & Standora, E. A. (2005). Western North Atlantic waters: Crucial developmental habitat for Kemp's ridley and loggerhead sea turtles. *CHELONIAN CONSERVATION AND BIOLOGY*, *4*(4), 872–882.

Moyer, A. E., Zheng, W., & Schweitzer, M. H. (2016). Keratin durability has implications for the fossil record: Results from a 10 year feather degradation experiment. *PLoS ONE*, *11*(7), 1–18. https://doi.org/10.1371/journal.pone.0157699

Mullineaux, L. S., & Garland, E. D. (1993). Larval recruitment in response to manipulated field flows. *Marine Biology: International Journal on Life in Oceans and Coastal Waters*, *116*(4), 667–683. https://doi.org/10.1007/BF00355484

Ostermann, A. I., Müller, M., Willenberg, I., & Schebb, N. H. (2014). Determining the fatty acid composition in plasma and tissues as fatty acid methyl esters using gas chromatography - a comparison of different derivatization and extraction procedures. *Prostaglandins Leukotrienes and Essential Fatty Acids*, *91*(6), 235–241. https://doi.org/10.1016/j.plefa.2014.10.002

Palaniappan, P. (2007). *The carapacial scutes of hawksbill turtles (Eretmocheyls imbricata): development, growth dynamics and utility as an age indicator* (pp. 1–358).

Petropoulos, G. P., Pandazaras, C. N., & Davim, J. P. (2010). Surface texture

characterization and evaluation related to machining. *Surface Integrity in Machining*, 37–66. https://doi.org/10.1007/978-1-84882-874-2_2

Piacenza, J., Piacenza, S., Mayoral, S., Kenney, A., & Shields, N. (2018). Design Opportunities for Sea Turtle Satellite Tracking Devices. *Volume 4: 23rd Design for Manufacturing and the Life Cycle Conference; 12th International Conference on Micro- and Nanosystems*, *4*. https://doi.org/10.1115/DETC2018-85583

Plotkin, P. (2010). Nomadic behaviour of the highly migratory olive ridley sea turtle Lepidochelys olivacea in the eastern tropical Pacific Ocean. *Endangered Species Research*, *13*(1), 33–40. https://doi.org/10.3354/esr00314

Polat, S., & Ozogul, Y. (2008). Biochemical composition of some red and brown macro algae from the Northeastern Mediterranean Sea. *International Journal of Food Sciences and Nutrition*, *59*(7–8), 566–572. https://doi.org/10.1080/09637480701446524

Riffel, A., Lucas, F., Heeb, P., & Brandelli, A. (2003). Characterization of a new keratinolytic bacterium that completely degrades native feather keratin. *Archives of Microbiology*, *179*(4), 258–265. https://doi.org/10.1007/s00203-003-0525-8

Robinson, D. P., Jabado, R. W., Rohner, C. A., Pierce, S. J., Hyland, K. P., & Baverstock, W. R. (2017). Satellite tagging of rehabilitated green sea turtles Chelonia mydas from the United Arab Emirates, including the longest tracked journey for the species. *PLoS ONE*, *12*(9), 1–19. https://doi.org/10.1371/journal.pone.0184286

Salmon, M., & Scholl, J. (2014). Allometric growth in juvenile marine turtles: Possible role as an antipredator adaptation. *Zoology*, *117*(2), 131–138. https://doi.org/10.1016/j.zool.2013.11.004

Schofield, G., Katselidis, K., Dimopoulos, P., Pantis, J., & Hays, G. (2006). Behaviour analysis of the loggerhead sea turtle Caretta caretta from direct in-water observation. *Endangered Species Research*, *2*(December), 71–79. https://doi.org/10.3354/esr002071

Seaborn, G. T., Katherine Moore, M., & Balazs, G. H. (2005). Depot fatty acid composition in immature green turtles (Chelonia mydas) residing at two near-shore foraging areas in the Hawaiian Islands. *Comparative Biochemistry and Physiology Part B: Biochemistry and Molecular Biology*, *140*(2), 183–195. https://doi.org/10.1016/J.CBPC.2004.09.017

Seney, E. (2008). Population dynamics and movements of the Kemp's ridley sea turtle, Lepidochelys kempii, in the northwestern Gulf of Mexico. *Population (English Edition), December*.

Seney, E., Higgins, B., & Landry, A. (2010). Satellite transmitter attachment techniques for small juvenile sea turtles. *Journal of Experimental Marine Biology and Ecology*, *384*(1–2), 61–67. https://doi.org/10.1016/j.jembe.2010.01.002

Seney, E., & Landry, A. (2011). Movement patterns of immature and adult female

Kemp's ridley sea turtles in the northwestern Gulf of Mexico. *Marine Ecology Progress Series*, *440*(Shaver 2010), 241–254. https://doi.org/10.3354/meps09380

Shaver, D. J., Hart, K. M., Fujisaki, I., Bucklin, D., Iverson, A. R., Rubio, C., Backof, T. F., Burchfield, P. M., Miron, R. D. J. G. D., Dutton, P. H., Frey, A., Peña, J., Gamez, D. G., Martinez, H. J., & Ortiz, J. (2017). Inter-nesting movements and habitat-use of adult female Kemp's ridley turtles in the Gulf of Mexico. *PLoS ONE*, *12*(3), 1–27. https://doi.org/10.1371/journal.pone.0174248

Shi, W., & Dumont, M. J. (2014). Review: Bio-based films from zein, keratin, pea, and rapeseed protein feedstocks. In *Journal of Materials Science* (Vol. 49, Issue 5, pp. 1915–1930). Springer. https://doi.org/10.1007/s10853-013-7933-1

Shoop, C. R., & Kenney, R. D. (1992). Seasonal Distributions and Abundances of Loggerhead and Leatherback Sea Turtles in Waters of the Northeastern United States. *Herpetological Monographs*, *6*, 43. https://doi.org/10.2307/1466961

Sloan, K., Zardus, J. D., & Jones, M. L. (2014). Substratum fidelity and early growth in Chelonibia testudinaria, a turtle barnacle especially common on Debilitated loggerhead (Caretta caretta) sea turtles. *Bulletin of Marine Science*, *90*(2), 581–597. https://doi.org/10.5343/bms.2013.1033

Solomon, S. E., Hendrickson, J. R., & Hendrickson, L. P. (1986). The structure of the carapace and plastron of juvenile turtles, Chelonia mydas (the green turtle) and Caretta caretta (the loggerhead turtle). *Journal of Anatomy*, *VOL. 145*, 123–131. http://www.scopus.com/inward/record.url?eid=2-s2.0-0022554154&partnerID=40&md5=19be1569d78aa653377f3ce797c4394c

Stauffer, E., Dolan, J. A., Newman, R., Stauffer, E., Dolan, J. A., & Newman, R. (2008). Gas Chromatography and Gas Chromatography—Mass Spectrometry. *Fire Debris Analysis*, 235–293. https://doi.org/10.1016/B978-012663971-1.50012-9

Stein, D. F. (1967). The Effect of Orientation and Impurities on the Mechanical Properties of Molybdenum Single Crystals. *Canadian Journal of Physics*, *45*(2), 1063–1074. https://doi.org/10.1139/p67-078

Stoneburner, D. L. (1982). Satellite Telemetry of Loggerhead Sea Turtle Movement in the Georgia Bight. *Copeia*, *1982*(2), 400. https://doi.org/10.2307/1444621

Tang, F., Gianola, D. S., Moody, M. P., Hemker, K. J., & Cairney, J. M. (2012). Observations of grain boundary impurities in nanocrystalline Al and their influence on microstructural stability and mechanical behaviour. *Acta Materialia*, *60*(3), 1038–1047. https://doi.org/10.1016/j.actamat.2011.10.061

Théberge, M. C., Prévost, D., & Chalifour, F. P. (1996). The effect of different temperatures on the fatty acid composition of Rhizobium leguminosarum bv. viciae in the faba bean symbiosis. *New Phytologist*, *134*(4), 657–664. https://doi.org/10.1111/j.1469-8137.1996.tb04931.x

Thums, M., Whiting, S. D., Reisser, J. W., Pendoley, K. L., Pattiaratchi, C. B., Harcourt, R. G., McMahon, C. R., & Meekan, M. G. (2013). Tracking sea turtle hatchlings - A

pilot study using acoustic telemetry. *Journal of Experimental Marine Biology and Ecology*, *440*, 156–163. https://doi.org/10.1016/j.jembe.2012.12.006

Ulmer, C. Z., Jones, C. M., Yost, R. A., Garrett, T. J., & Bowden, J. A. (2018). Optimization of Folch, Bligh-Dyer, and Matyash sample-to-extraction solvent ratios for human plasma-based lipidomics studies. *Analytica Chimica Acta*, *1037*, 351–357. https://doi.org/10.1016/j.aca.2018.08.004

van den Berg, R. A., Hoefsloot, H. C. J., Westerhuis, J. A., Smilde, A. K., & van der Werf, M. J. (2006). Centering, scaling, and transformations: Improving the biological information content of metabolomics data. *BMC Genomics*, *7*, 1–15. https://doi.org/10.1186/1471-2164-7-142

Vander Zanden, H. B., Bjorndal, K. A., Reich, K. J., & Bolten, A. B. (2010). Individual specialists in a generalist population: results from a long-term stable isotope series. *Biology Letters*, *6*(5), 711–714. https://doi.org/10.1098/rsbl.2010.0124

Varo-Cruz, N., Hawkes, L. A., Cejudo, D., López, P., Coyne, M. S., Godley, B. J., & López-Jurado, L. F. (2013). Satellite tracking derived insights into migration and foraging strategies of male loggerhead turtles in the eastern Atlantic. *Journal of Experimental Marine Biology and Ecology*, *443*, 134–140. https://doi.org/10.1016/j.jembe.2013.02.046

Velioglu, S. D., Temiz, H. T., Ercioglu, E., Velioglu, H. M., Topcu, A., & Boyaci, I. H. (2017). Use of Raman spectroscopy for determining erucic acid content in canola oil. *Food Chemistry*, *221*, 87–90. https://doi.org/10.1016/j.foodchem.2016.10.044

Vetter, W., Darwisch, V., & Lehnert, K. (2020). Erucic acid in Brassicaceae and salmon – An evaluation of the new proposed limits of erucic acid in food. *NFS Journal*, *19*, 9–15. https://doi.org/10.1016/j.nfs.2020.03.002

Wahl, M., & Lafargue, F. (1990). Marine epibiosis. *Oecologia*, *82*(2), 275–282. https://doi.org/10.1007/bf00323545

Wang, B., & Sullivan, T. N. (2017). A review of terrestrial, aerial and aquatic keratins: the structure and mechanical properties of pangolin scales, feather shafts and baleen plates. *Journal of the Mechanical Behavior of Biomedical Materials*, *76*(April), 4–20. https://doi.org/10.1016/j.jmbbm.2017.05.015

Wang, B., Yang, W., McKittrick, J., & Meyers, M. A. (2016). Keratin: Structure, mechanical properties, occurrence in biological organisms, and efforts at bioinspiration. *Progress in Materials Science*, *76*, 229–318. https://doi.org/10.1016/j.pmatsci.2015.06.001

Watson, K., & Granger, R. (1998). Hydrodynamic effect of a satellite transmitter on a juvenile green turtle (Chelonia mydas). *Journal of Experimental Biology*, *201*(17), 2947–2505.

Weedon, B., & Moss, G. (1995). Structure and nomenclature. *Carotenoids, Vol. 1A, Isolation and Analysis*, 27–70.

Welch, D. W., Melnychuk, M. C., Rechisky, E. R., Porter, A. D., Jacobs, M. C.,

Ladouceur, A., McKinley, R. S., & Jackson, G. D. (2009). Freshwater and marine migration and survival of endangered Cultus Lake sockeye salmon (Oncorhynchus nerka) smolts using POST, a large-scale acoustic telemetry array. *Canadian Journal of Fisheries and Aquatic Sciences*, *66*(5), 736–750. https://doi.org/10.1139/F09-032

White, G. C., & Garrott, R. A. (1990). *Analysis of wildlife radio-tracking data*. Academic Press.

Williams, W. S. (1964). Influence of temperature, strain rate, surface condition, and composition on the plasticity of transition-metal carbide crystals. *Journal of Applied Physics*, *35*(4), 1329–1338. https://doi.org/10.1063/1.1713614

Wilson, B., Hammond, P. S., & Thompson, P. M. (1999). Estimating size and assessing trends in a coatal bottlenose dolphin population. *Ecological Applications*, *9*(1), 288–300. https://doi.org/10.1890/1051-0761

Wilson, R., Grémillet, D., Syder, J., Kierspel, M., Garthe, S., Weimerskirch, H., Schäfer-Neth, C., Scolaro, J., Bost, C., Plötz, J., & Nel, D. (2002). Remote-sensing systems and seabirds: their use, abuse and potential for measuring marine environmental variables. *Marine Ecology Progress Series*, *228*, 241–261. https://doi.org/10.3354/meps228241

Wood, C. J. (1998). Movement of bottlenose dolphins around the south-west coast of Britain. *Journal of Zoology*, *246*(2), 155–163. https://doi.org/10.1017/S0952836998010048

Worley, B., & Powers, R. (2012). Multivariate Analysis in Metabolomics. *Current Metabolomics*, *1*(1), 92–107. https://doi.org/10.2174/2213235x130108

Wyneken, J. (1988). *Comparative and functional considerations of locomotion in turtles* [University of Illinois]. https://elibrary.ru/item.asp?id=5952859

Yeon, J., Song, Y., Kim, K. K., & Kang, J. (2019). Effects of epoxy adhesive layer thickness on bond strength of joints in concrete structures. *Materials*, *12*(15), 1–10. https://doi.org/10.3390/ma12152396

Zhai, L. L., Ling, G., Li, J., & Wang, Y. (2006). The effect of nanoparticles on the adhesion of epoxy adhesive. *Materials Letters*, *60*(25–26), 3031–3033. https://doi.org/10.1016/j.matlet.2006.02.038

Zhai, L. L., Ling, G. P., & Wang, Y. W. (2008). Effect of nano-Al2O3 on adhesion strength of epoxy adhesive and steel. *International Journal of Adhesion and Adhesives*, *28*(1–2), 23–28. https://doi.org/10.1016

APPENDICES

APPENDIX A. OVERVIEW OF FAP

Fatty acid methyl esters (FAMEs) are a derived form of fatty acids that may be extracted from tissue samples as free fatty acids or as the fatty acid tails from a variety of lipids, such as triglycerides or phospholipids. The Bligh-Dyer method, one of the most common extraction methods, utilizes a biphasic system to non-selectively extract lipids from cells (Bligh & Dyer, 1959; Ulmer *et al.*, 2018). During acid-catalyzed reactions in the presence of methanol, fatty acid chains are first separated from glycerol backbones through hydrolysis with the resultant free fatty acids then methylated in a process termed transesterification (Weedon & Moss, 1995). Since FAMEs are volatile and non-polar, they may be used in gas chromatography—a technique used to separate and analyze volatile compounds based on their boiling point, vapor pressure, and polarity (Stauffer *et al.*, 2008).

Keratin scute samples were collected and processed as detailed in Objective 1, then stored in a –80 ºC freezer. Scute samples were cryo-milled (RETSCH GmbH, Haan Germany) for pulverization and homogenization with liquid nitrogen to preserve scute chemical integrity while processing. Scute powder was transferred to individual cryovials and stored in a –80 ºC freezer. Excess material for each scute subsample was collected for a "pooled" quality control material. Pooled samples were used in part for method development, which consisted of optimizing the following values: mass of scute powder (mg), internal standard solution volume (µL), reconstitution volume (mL), and injection volume (µL).

Extraction

Fatty acids were extracted and derivatized following procedures detailed by Bligh & Dyer (1959) and Ostermann *et al.* (2014), respectively. Into individual 20-mL glass test tubes (Fisher, Waltham, MA) with a PTFE-lined cap, 100 mg of scute powder of each scute subsample or 20 mg of quality control material (NIST SRM 1947, Lake Michigan fish tissue) were weighed (0.00001 g precision) with an analytical balance (Mettler Toledo Excellence Plus XP205, Columbus, OH). Three mL of extraction solution (2:1 MeOH:$CHCl_3$) were added to each test tube. Six µL of internal standard (ISTD) solution (1.0842 mg/g (ppth) C13:0 triglyceride, Nu-Check Prep, Elsyian, MN) were added to each scute sample and 20 µL of ISTD solution were added to each standard reference material (SRM) sample and the mass recorded (0.00001 g precision). One mL of chloroform (HPLC grade, Fisher, Waltham, MA) followed by 1.8 mL of 18-MΩ water was added to each test tube using a Mohr pipette and micropipettor, respectively. Test tubes were vortexed for 20 s, then centrifuged (International Equipment Company Centra CL13) at 3,000 rpm for 10 min. Using a 2-mL disposable Pasteur pipette, the bottom (organic) layer was removed and transferred to a new test tube. The remaining aqueous layer was washed with 3 mL of chloroform. Test tubes were again vortexed and then centrifuged. The bottom layer was likewise removed and transferred to the new test tube mentioned above. Test tubes were blown down with nitrogen at 40 ºC at 15 psi in an evaporator (Biotage Concentration Workstation

TurboVap LV, Uppsala, Sweden). Additionally, a method blank was created with 100 mg of 18-MΩ water. The method blank and all quality controls were extracted in triplicate.

Derivatization

Upon removal from the evaporator, test tubes were reconstituted with 250 µL of hexane (GC Resolve grade, Fisher, Waltham, MA), followed by 600 µL of derivatizing solution (methyl acetate, 1:9, Sigma, St. Louis, MO). After vortexing for 10 s, test tubes were tightly capped then heated in an oven (Fisher Model 230F Isotemp, Waltham, MA) at 95 ºC for 1 h. Test tubes were removed and allowed to cool to room temperature for 10 min. Subsequently, 0.750 mL of potassium carbonate solution (0.440 M, Sigma, St. Louis, MO) was added to each test tube to neutralize the reaction. Test tubes were vortexed for five seconds, then centrifuged at 3,000 rpm for 10 min. Using a micropipettor, 75 µL of the hexane layer was transferred to an autosampler vial with PTFE-lined caps and vial insert. Autosampler vials were then loaded onto the autosampler in random order and analyzed by the GC-FID instrument.

A gas chromatograph with flame ionization detector (GC-FID) (6890N, Agilent, Santa Clara, CA, USA), an Rt-2560 GC column (100 m × 0.25 mm, 0.20-µm film thickness, Restek, Bellefonte, PA, USA) with a deactivated guard column (Siltek 10026, 5 m × 0.25 mm, Restek, Bellefonte, PA, USA) and wool-packed, focusing split liner (210-4004-5, Agilent , Santa Clara, CA, USA) was used for all experiments. Oven gradient was: initial 100 °C, hold 4 min; ramp 3.0 °C/min; final 240 °C, hold 15 min. Other parameters were injector and detector temperatures at 225 °C and 285 °C, respectively; 2-µL injection volume; split ratio, 24:1; with helium as carrier gas at constant flow, 1.0 mL/min and velocity, 18 cm/s.

FAME standards mix (GLC-463 Nu-Chek Prep, Elysian, MN, USA) supplemented with FAMEs of C18:2*n*-9 (1256, Matreya, State College, PA, USA); C21:0 (N-21-M, Nu-Chek Prep); C22:1*n*-9 (U-80-M, Nu-Chek Prep); C22:5*n*-6 (U-102-M, Nu-Chek Prep) were used for retention times alignments. Internal standard solution of C13:0 triglyceride (Nu-Chek Prep, T-135) was added pre-extraction. National Institute of Science Technology (NIST) SRM 1947 Lake Michigan Fish Tissue (muscle) was used as a validation and quality control material.

APPENDIX B. FRICTION COEFFICIENTS

Friction coefficients for droplets of three liquids (distilled water, chlorohexidine, and vegetable oil) on both plexiglass and loggerhead sea turtle scute subsamples remaining from Objective 1 were computed in a laboratory setting. Stratified random sampling was employed to select five loggerhead sea turtle scute subsamples that were (a) intact (*i.e.*, no visible holes), and (b) free of residual epoxy. Selected scute subsamples were flattened and mounted via tape to a plexiglass backboard. Prior to the start of trials, the distance over which the droplets would travel was measured for all scute samples. To standardize distance travelled for plexiglass replicates, the mean distance travelled (cm) for scute subsamples was marked via tape on each plexiglass replicate. Scute subsamples and plexiglass replicates were clamped to a flat surface at a 90º angle. One drop (approximately 0.1 mL) of each liquid was placed with a 1-mL syringe on the top of each replicate. The time (0.01 s precision) required for the droplet to travel the measured distance was recorded manually. Five loggerhead sea turtle subsamples and five plexiglass replicates (20 cm × 23 cm) were tested five times each, with subsequent droplets placed approximately 1 cm apart to avoid overlapping paths. The rate each droplet travelled was calculated for all replicates, and descriptive statistics were computed to characterize variability. The friction coefficient for loggerhead sea turtle subsamples was calculated from the ratio of mean plexiglass rate and known friction coefficient to mean loggerhead sea turtle scute rate.

Results

Following preliminary trials using distilled water and chlorohexidine droplets, remaining trials were foregone due to loggerhead sea turtle scute subsamples absorbing the droplets prior to travelling the entire distance. Droplet testing for friction coefficients was the least reliable technique since it was dependent on the physical properties of the droplet liquid.

Mean distance travelled of vegetable oil droplets on loggerhead sea turtle subsamples was 5.8 cm (CV = 0.3). Droplets travelled at a mean rate of 0.24 cm/s (CV = 0.4) on loggerhead sea turtle subsamples and 0.20 cm/s (CV = 0.3) on plexiglass replicates. The calculated friction coefficient for loggerhead sea turtle subsamples was 0.96.

APPENDIX C. SMALL-SCALE EPOXY ADHESION TESTS

Small-scale epoxy adhesion tests were performed to address intra-material variability. To induce detachment, six substrates with consistent break forces were selected for further testing, with three replicates each. Epoxy application order was recorded to address the possibility that delays in epoxy application affect break force. Replicates were secured to a wooden weight tray on a modified force apparatus using a wooden mounting brace (1.4 cm thick) with a circular cut-out measuring 3.6 cm in diameter (Figure AC.1). Since no detachment occurred in previous trials with a maximum weight of 4.5 kg, trials began with 9.1 kg of weights added to the base of the weight tray on the force apparatus. At one-minute intervals, weights (4.5 kg) were systematically added to the base of the weight tray until detachment occurred, up to a maximum load of 63.5 kg and a maximum trial time of 20 minutes. The maximum break force (1 N precision) and trial duration (0.1 min precision) were recorded for each trial. A regression analysis was performed to test the effect of epoxy application order on break force. Descriptive statistics were used to characterize variability in force required to dislodge epoxy from substrate types. Subsequently, the two substrates with the highest and lowest mean maximum break force were selected to test seven additional replicates (10 total) per substrate to capture intra-material variability.

Fifteen additional replicates of laminate flooring were tested to explain intra-material variability by duration of epoxy curing. Three treatments of cure time (2, 6, and 70 h) consisted of five replicates each and were selected based on the minimum and maximum amount of time elapsed from epoxy application to initiation of trials. Epoxy adhesion tests were performed using methods described above. Descriptive statistics were used to characterize variability in force. A single-factor ANOVA was used to test the effect of cure time on break force.

Given intra-material variability was not explained by epoxy application or cure time, 10 replicates of both tile 2 and laminate flooring were tested to account for intra-replicate variability in break force. Following the first run, remaining epoxy was removed from replicates with a chisel before the second round of epoxy application. Epoxy adhesion tests were performed as previously described. For both runs, detachment type was categorized by whether the epoxy detached from the substrate (epoxy), or the eye-screw detached from the epoxy (screw). Descriptive statistics were used to characterize variability in force. A paired t-test was used to determine if break force significantly differed between first and second runs.

Small-scale epoxy adhesion tests were performed to quantify mean maximum break force for 25 replicates of the experimental unit substrate (tile 1). Descriptive statistics were calculated to capture intra-material variability. A two-factor ANOVA was performed to assess the effect of epoxy lot number and trial date on break force.

Results

No relationship was detected between mean maximum break force and epoxy application order for the six most consistent substrates ($r^2 = 0.08$; Figure AC.2). Of the six substrates, tile 2 ($n = 10$) had the highest mean maximum break force at 578 N (CV = 0.1), and laminate flooring ($n = 10$) had the lowest at 89 N (CV = 0.5).

Mean maximum break force was not significantly related to cure time ($P = 0.15$, $df = 14$). Intra-material variability in break force could not be explained by either order of epoxy application or cure time. Inconsistent break forces suggest substrate has more impact on epoxy bonding than either delays in epoxy application or cure time.

Mean maximum break force significantly decreased from the first run to the second for both tile 2 ($P < 0.05$, $df = 9$; Figure AC.3a) and laminate flooring ($P < 0.001$, $df = 9$; Figure AC.3b). Detachment type generally shifted by run from epoxy to screw for tile 2, but did not change for laminate flooring. Inconsistency between runs for the same replicate suggests removal of remaining epoxy between runs may allow stronger epoxy bonding to substrates due to increased surface roughness, and may induce screw detachment rather than epoxy detachment.

Mean maximum break force for tile 1 was 380 N (CV = 0.5, $n = 25$). Ten replicates assembled with epoxy lot 330 had a mean break force of 540 N (CV = 0.2). Fifteen replicates assembled with epoxy lot 262 had a mean break force of 280 N (CV = 0.4). Of the 25 total replicates, 15 replicates ran on 11 June had a mean break force of 500 N (CV = 0.3), and 10 replicates ran on 13 June had a mean break force of 210 N (CV = 0.2). Break force was significantly affected by both epoxy lot number ($P < 0.001$, $df = 1$) and trial date ($P < 0.005$, $df = 1$).

Figure AC.1. Front view of the force apparatus employed in small-scale testing with one 4.5 kg weight loaded onto bottom weight tray. Replicates were secured onto force apparatus by a wooden brace with a circular cut-out measuring 3.6 cm in diameter, and mounted by eye-screw.

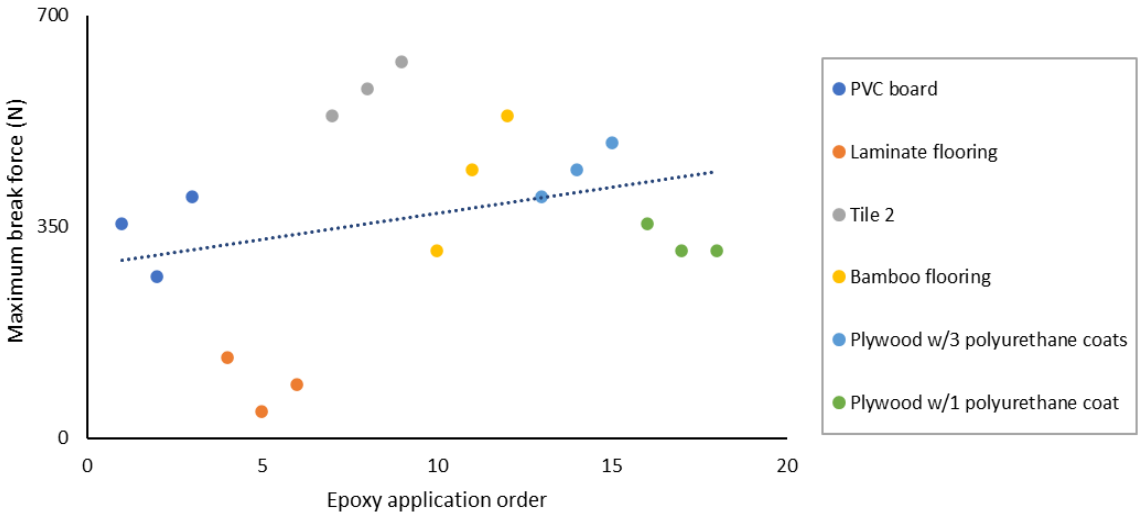

Figure AC.2. Maximum break force (y-axis) by epoxy application order (x-axis) for each of three replicates of various substrate types (color). Blue dashed line corresponds to linear trendline for all replicates (n = 18) across substrate types.

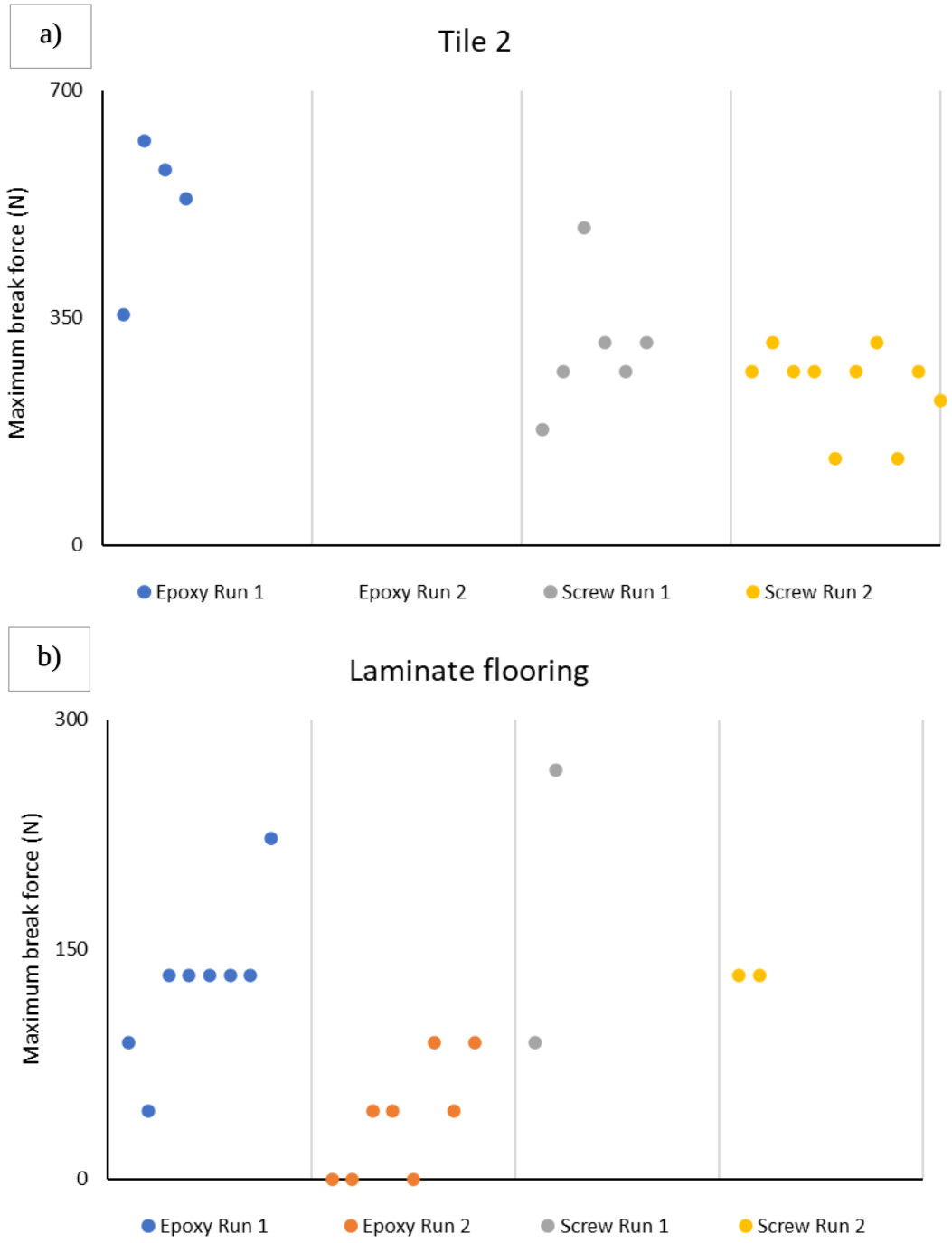

Figure AC.3. Maximum break forces (y-axes) by detachment type (epoxy or screw) and run (x-axes) for a) tile 2, and b) laminate flooring.

APPENDIX D. CARAPACE ANGLE

Two angles (0º and 30º) were tested representing the minimum and maximum carapace angles for either species. Two morphometric measurements recorded for loggerhead sea turtles and Kemp's ridley sea turtles captured by the SCDNR in-water sea turtle trawl survey (2000 to 2018) were used to test the null hypothesis of no difference in carapace morphology between species. Minimum straight-line carapace length (SCLmin, 0.1 cm precision) and body depth (0.1 cm precision) measured with tree calipers (Haglöf Mantax Blue, Sweden) were used to compute carapace slope. Carapace slopes were used to compute the angle of the slopes in radians using the arctangent formula in MS Excel, then converted to degrees using the degrees formula in MS Excel. Given that loggerhead sea turtles comprise 90% of sea turtles captured in the SCDNR survey, a percentile distribution of carapace angles was computed to standardize the amount of input data for analysis per species. Following removal of outliers in each percentile distribution, a test for normality was performed and appropriate statistical test selected to compare distributions.

Results

After removing outliers, percentile distributions of carapace angle were non-normal; therefore, non-parametric statistical testing was selected. A significant difference was detected (Kruskal-Wallis stat = 46.26, $P < 0.005$, df = 1; Figure AD.1) between species with greater carapace angles for loggerhead sea turtles (19.0 to 27.5º, median = 22.3º, n = 2,248) than for Kemp's ridley sea turtles (18.4 to 28.1º, median = 20.9º, n = 354).

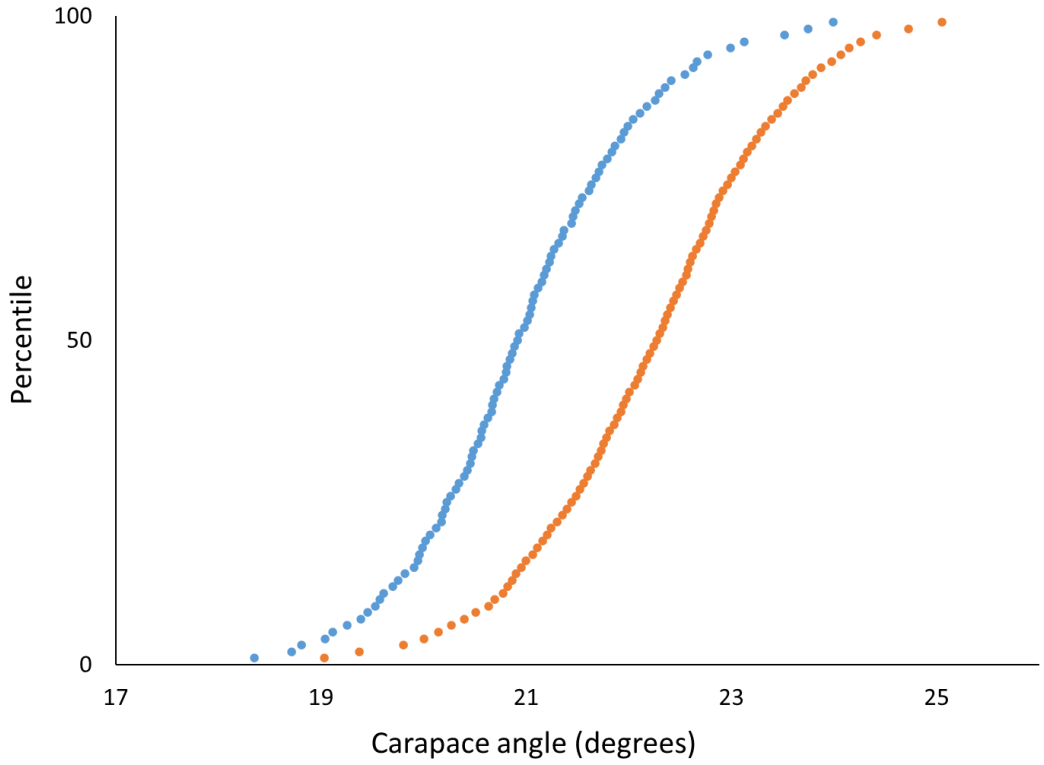

Figure AD.1. Percentile distribution of carapace angles for loggerhead sea turtles (orange) and Kemp's ridley sea turtles (blue).

APPENDIX E. FRAME CONSTRUCTION

Six frames measuring 1.12 m × 0.91 m were constructed from galvanized powder-coated steel multi-purpose fence panels (11.0 cm × 5.0 cm mesh, Ironcraft). Treatments consisted of small (n = 20) and large (n = 19) surrogate transmitters. Frames 1–3 hold three small and three large pre-assembled replicates; small replicates were randomly assigned to even positions 1–6, and large replicates were randomly assigned to odd positions 1–6 (MS excel random number generator; Figure AE.1a). Frames 4–5 hold four small and three large replicates; small replicates were randomly assigned to even positions 1–6 and position 7, and large replicates were randomly assigned to odd positions 1–6 (MS excel random number generator; Figure AE.1b). Frame 6 holds three small and four large replicates; small replicates were randomly assigned to positions 2, 4, or 7, and large replicates were randomly assigned to positions 1, 3, 5, or 6 (MS excel random number generator; Figure AE.1b). Nylon cable ties were used to secure the corner of each replicate to the frame. For stability and ease of securing frames to seafloor, frames rested on PVC (3.81 cm diameter) tracks approximately 3.1 m in length. Two lengths of PVC support one row of three frames, with two rows total to accommodate six frames. Rebar posts (1.9 cm diameter) was driven through holes (2.54 cm diameter) in the PVC into the seafloor at each corner of the track (Figure AE.2). Frames were secured to PVC tracks via nylon cable ties.

One frame measuring 1.12 m × 0.91 m was constructed from galvanized powder-coated steel multi-purpose fence panels (11.0 cm × 5.0 cm mesh, Ironcraft). Treatments consisted of no angle (n = 20) and 30º (n = 20) replicates, with replicates randomly assigned to positions 1–40 (MS excel random number generator; Figure AE.3). The first row of each frame was randomly assigned to either no angle or 30º, with alternating subsequent rows. To simulate a carapace angle of 30º, replicates were secured to wooden supports (30 cm × 1.9 cm × 4 cm; length × width × height) cut at a 30º angle via nylon cable ties. Wooden supports received three coats of fast-drying polyurethane clear gloss (Minwax), and were then coated with anti-fouling paint (Rust-oleum Marine Coatings Boat Bottom). Holes were drilled through the center edges of opposite ends of each replicate, through which nylon cable ties were used to secure units to the frame. The frame was fastened to PVC tracks approximately 1.02 m in length and secured with rebar posts to the seafloor as previously described.

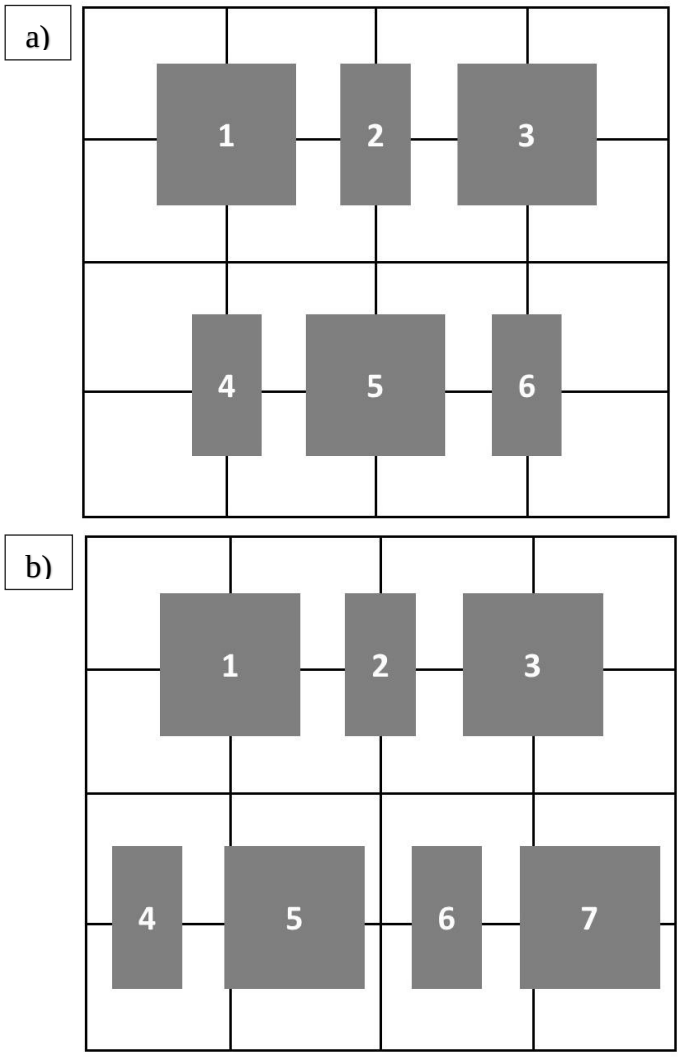

Figure AE.1. Experimental design for randomly assigning replicates to frames, with a) three frames each consisting of three small and three large replicates randomly assigned to positions (gray), and with b) three frames each consisting of either four small and three large replicates, or three small and four large replicates.

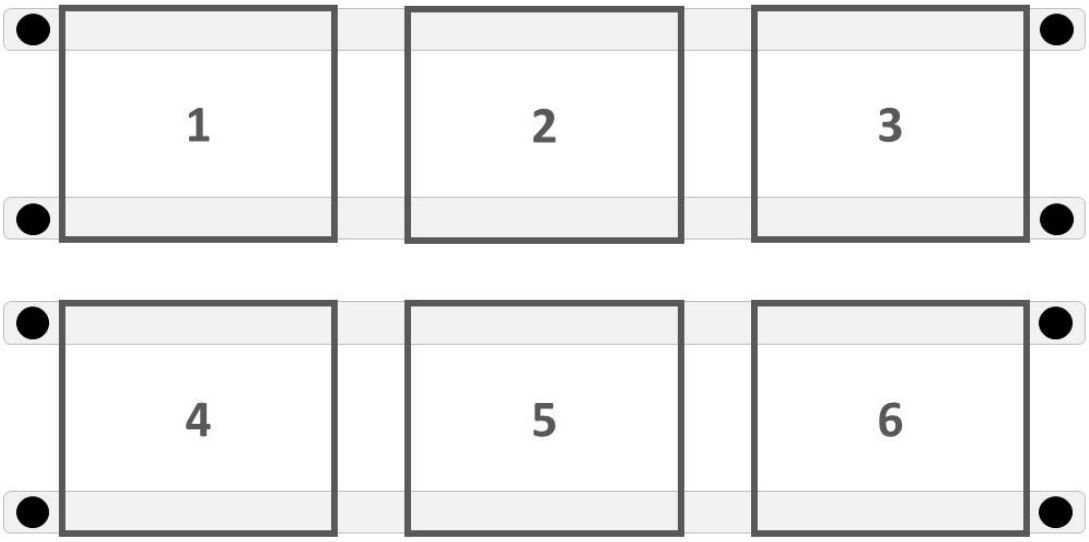

Figure AE.2. Schematic of frame layout on seafloor. Frames (1–6) rested on PVC (light gray) tracks. Rebar posts were driven through holes (black) in the PVC into the seafloor. Frames were secured to PVC tracks via nylon cable ties.

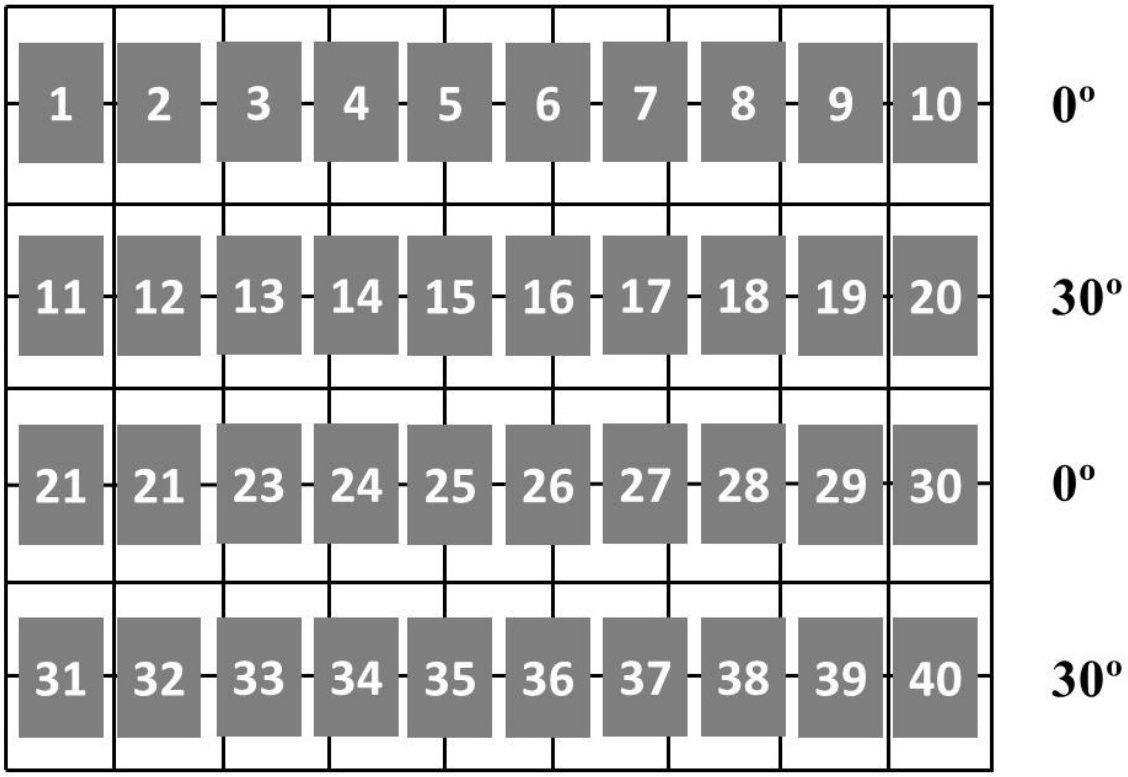

Figure AE.3. Experimental design with replicates randomly assigned to positions (gray) on alternating flat-angled rows.